Review of Dielectrophoretic Manipulation of Micro and Nanomaterials: Fundamentals, Recent Developments, and Challenges

Taher Ghomian, Senior Member, IEEE, Joshua Hihath, Senior Member, IEEE

Abstract— This paper reviews the state-of-the-art methods of dielectrophoresis for micro- and nanomaterial manipulation. Dielectrophoresis is a well-known technique for material manipulation using a nonuniform electric field. This field can apply a force to dielectric materials and move them toward a predefined location. Controlling the pattern of the electric field and its intensity, achieved by a specific arrangement of electrodes or insulators, along with the dielectric properties of the materials allows a variety of manipulation functions including trapping, and transportation. The development separation. microfabrication techniques has significantly improved the research quality in the field of dielectrophoresis for precisely manipulating micro and nanomaterials. Later, the advent of microfluidic devices provided an excellent platform for reliable and practical devices. Modifying the shape, geometry, and material of the electrodes, isolating the electrodes from the sample, incorporating a particular arrangement of insulators within the electric field, and monitoring the operation in situ are some of the methods utilized for overcoming common problems in dielectrophoretic devices or the problems associated with a specific sample and the manipulation function. The goal of the research in this field is to design practical, high throughput, and inexpensive devices that reliably manipulate micro and nanomaterials. Accordingly, this review aims to represent latest findings and advancements in the field of dielectrophoresis. In particular, the working principles, technical implementation details, current status, and the issues and challenges of dielectrophoretic devices for electrode-based and insulator-based dielectrophoresis in terms of operation and fabrication are discussed.

Index Terms— Dielectrophoresis, dielectrophoretic manipulation, microparticles, nonuniform electric field, nanomaterials, separation, trapping, transportation.

I. INTRODUCTION

Discrete by Herbert Pohl in 1951 when he noticed the motion of suspended particles as a result of an applied inhomogeneous electric field [2]. He conducted a preliminary test by applying high voltages, in the range of 10 kV, to generate sufficient electric fields for the experiment. Although this level of the applied voltage prevented having practical DEP devices for most applications, later in the 1990s

This work was supported in part by the U.S. National Science Foundation (1807555 and 2036865).

microfabrication techniques significantly improved the situation. Since these microsystems require much lower voltages for operation, useful and practical DEP microdevices have been developed [3]. Recently, micro and nanomaterials are increasingly being used in many applications such as biology [4-6], energy harvesting [7-10], agriculture [11, 12], optoelectronics [13, 14], nanoelectronics [15-18], and chemistry [19-21]. As such, DEP provides an intriguing and important platform for manipulating micro and nanostructures for different purposes.

There are quite a few established methods to manipulate micro and nanostructures. Optical tweezers [22], dielectrophoresis [23], hydrodynamic flow [24], and acoustic controls [25] are well-known and widely applied manipulation techniques. Optical tweezers, as a noninvasive technique, are suitable for a wide range of applications such as manipulating biomaterials, [26] and they can be integrated on a chip using a high throughput microfabrication process to develop practical devices [27, 28]. However, this technique suffers from low efficiency and the manipulation process is challenging when dealing with nanomaterials. To enhance the performance of optical tweezers some complicated measurements are required [29] which increases the cost and the complexity of the fabrication process. Hydrodynamic flow, as another technique, is a low-cost, high efficiency, noninvasive, and easily operated approach for particle confinement in microfluidic structures [30]. Nevertheless, it is challenging to have high throughput and high resolution manipulation simultaneously [31, 32]. Another frequently reported method is utilizing acoustic waves to immobilize objects in the pressure minima of standing acoustic waves inside a microfluidic channel [33]. Although this technique can quickly and efficiently trap and manipulate particles, the operation is not simple and it is known as an invasive technique. As such, it has a limited applications compared with the other methods. Importantly however, this method can be readily applied to soft materials such as biomedical species.

The discussed methods have concentrated mostly on manipulating particles inside a solution. Studying the properties of an individual particle or a few particles demands further capabilities to align the materials in a particular direction (for non-symmetrical particles) and attach them to a pair of electrodes. This can be achieved by using the DEP technique which is based on the movement of a dielectric

T. Ghomian is with Marshall University, Huntington, WV, USA. J. Hihath is with the University of California, Davis, CA, USA (correspondence e-mail: ghomian@marshall.edu).

material in a non-uniform electric field. Particle moving based on electrical fields is a promising technique for manipulating micro and nanostructures or immobilizing them at accurate locations of interest [34-39] and studying the properties of the objects. Since the DEP technique is fast, noninvasive, and accurate, it can play an important role in trapping, separating, and transporting micro and nanomaterials such as biological samples. In addition, DEP provides options for massively parallel and high-speed manipulation in a miniaturized device since only a small volume of sample is needed [40]. Moreover, DEP is compatible with microfabrication technology and therefore the development of DEP arrays capable of simultaneous manipulation of many particles in a single device is achievable [41]. As such, DEP provides a unique platform for more accurate manipulation, particle immobilization out of an aqueous medium for characterization as well as high miniaturization factor.

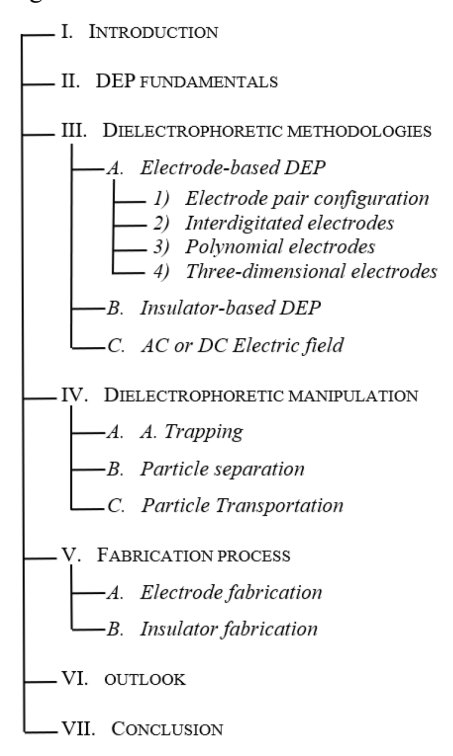


Fig. 1. General diagram of the content and structure

Accordingly, this review intends to provide an overview of the recent developments, experimental approaches, fabrication processes, and challenges in manipulating DEP devices. As shown in Fig. 1, in section 2, we introduce the fundamentals and background of the DEP phenomenon. Then recent developments and challenges of the DEP technique from the point of creating appropriate electric fields are studied in section 3. In this section, we introduce popular configurations and considerations useful for generating nonuniform electric fields suitable for material manipulation. Section 4 focuses on the manipulation functions including trapping, separation, and transportation. Section 5 concentrates on the review of the DEP device fabrication processes for different configurations and their related challenges. Finally, we summarize the

general requirements of DEP devices and correlate them to the required future research in the last section of the paper.

II. DEP FUNDAMENTALS

DEP refers to a phenomenon in which a force is applied to a polarizable object when it is placed in a non-uniform electric field [4]. This force can migrate the particle toward the intensive region of the electric field (toward the field gradient) or away from the intensive region of the electric field (away from the field gradient) depending on the dielectric properties of the object and suspending media [42].

There are many thorough reviews of the fundamentals of dielectrophoresis in the literature [43-45], therefore here we will briefly explain the mentioned phenomenon. If a polarizable particle is exposed to an electric field, charges with appropriate polarities are accumulated on both sides of the material at its surface, as shown in Fig. 1(a), as the established electric field inside the particle opposes the external electric field. As such, the Coulomb force F=qE is applied to both sides of the particle. If the electric field is uniform the Coulomb force acting on both sides of the particle is equal in magnitude but opposite in direction, thus canceling each other out, and resulting in zero net force ($\mathbf{F} = \mathbf{q}^{+}\mathbf{E} - \mathbf{q}^{-}\mathbf{E} =$ 0). In the case of a nonuniform electric field, as shown in Fig. 1(a), the story is slightly different. The Coulomb force acting on either side of the particle is in opposite direction but not equal in magnitude, therefore, the net force appearing on the particle is not zero and it is therefore capable of displacing the particle. For simplicity, let's consider a spherical particle located in a nonuniform electric field, as shown in Fig. 1(a) and (b). This nonuniform electric field can be generated by a pair of electrodes that are not similar in shape and size. As such, the particle is polarized, and positive and negative charges are separated by a distance d (diameter of the sphere). If the electric field at the negatively charged side of the particle is $\mathbf{E}(\mathbf{r})$, the net Coulomb force acting on the particle is given by Equation 1.

$$\mathbf{F} = q^{+}\mathbf{E}(\mathbf{r} + \mathbf{d}) - q^{-}\mathbf{E}(\mathbf{r}) \tag{1}$$

We assume that the size of the particle is small enough (this is a practical assumption since DEP devices are acting on micro and nanostructures), therefore we can apply the following equation:

$$E(r+d) = E(r) + d.\nabla E(r)$$
 (2)

Substituting Equation 2 in Equation 1 with some simple algebra gives the following equation:

$$\mathbf{F} = q\mathbf{d}.\,\nabla\mathbf{E}\tag{3}$$

This equation shows that the net force applied to a particle in a nonuniform electric field depends on the electric field gradient and is multiplied by the induced charge dipole length (qd) which is defined as dipole moment (m). If the electric field is not static and its magnitude and phase varies with time, such as when applying a sinusoidal electric field, the calculations show that the time-averaged DEP force acting on a spherical polarizable particle is given by [46, 47]:

$$\langle F_{DEP} \rangle = 2\pi \varepsilon_m r^3 Re[K(\omega)] \nabla E^2 \tag{4}$$

where $r, \varepsilon_m, \varepsilon_p^*, \varepsilon_m^*$, and E are the particle radius,

permittivity of the suspending media, complex permittivity of the particle, complex permittivity of the suspending media, and external electric field (root mean square value is used for AC electric field), respectively. $K(\omega)$ is called the Clausius-Mossotti factor and it is given by:

$$K(\omega) = \frac{\varepsilon_p^* - \varepsilon_m^*}{\varepsilon_p^* + 2\varepsilon_m^*} \tag{5}$$

Equation 4 illustrates that the magnitude of the DEP force linearly depends on the cubed radius of the particle, the permittivity of the suspending media, complex permittivity of the suspending media and particle which defines the real part of $K(\omega)$, and the gradient of the squared external electric field. This indicates that particles with the same materials $(\varepsilon_{p1}^* = \varepsilon_{p2}^*)$ and different sizes tolerate different DEP forces and accordingly the DEP force can be used to separate them by size inside a solution. Except for the Clausius-Mossotti factor, the other three factors are positive, therefore the direction of the applied DEP force depends on the sign of the real part of the Clausius-Mossotti factor. It can be inferred from Equation 4 that if the value of $Re[K(\omega)]$ is positive, the DEP force (F_{DEP}) acts toward the electric field gradient and moves particles toward the region of the highest electric field, as shown in Fig. 1(a). This is referred to as positive DEP (pDEP). On the other hand, if the value of $Re[K(\omega)]$ is negative, acting F_{DEP} force is in the opposite direction of the positive case and particle is repelled from the intensive region of the electric field and moves toward the low-intensity region of the electric field, as shown in Fig. 1(b). This is called negative DEP (nDEP). Fig. 1(c) shows a typical structure for pDEP to trap a particle in the high-intensity region of the electric field. The arrangement of electrodes is in such a way that the intensity of the electric field is maximum along the axis connecting two electrodes (deep red color) and decreases moving to either side of this axis. Particles in the blue region (low-intensity electric field) experience a pDEP force. This force attracts the particle toward the high-intensity field and when the particle reaches that region, it doesn't tolerate any field gradient, therefore, the net force on the particle is zero and it stops moving. If any force such as Brownian motion or vibration deviates the particle from the trap location, DEP force can act on the particle and return it to the trap location.

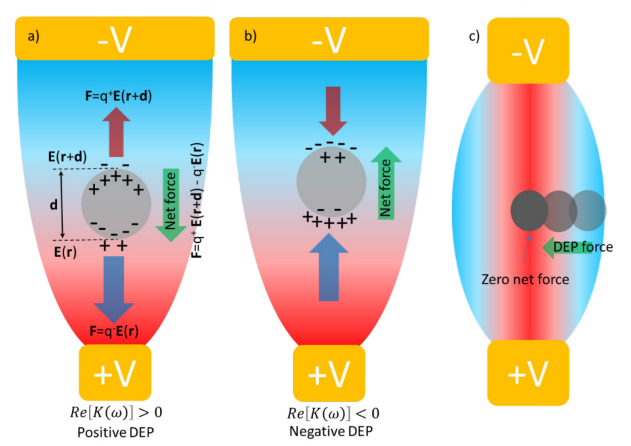


Fig. 1. Schematic diagram showing the effect of dielectrophoretic force acting on a particle located in a nonuniform electric field. Since Coulombic

forces acting on either side of the particle are not equal, (a) particle moves toward the field gradient (pDEP) as a result of the positive $Re[K(\omega)]$; (b) particle moves away from the field gradient (nDEP) as a result of the negative $Re[K(\omega)]$; (c) particle moves toward high electric field region until experiencing zero net force at maximum electric field region located on the axis connecting two electrodes.

The Clausius-Mossotti factor is frequency-dependent since the complex permittivity of materials is a function of frequency. Here we will describe the frequency-dependent behavior of the DEP force at two low frequency and high frequency operation regimes. The complex permittivities of particle and medium is defined as:

$$\varepsilon_p^* = \varepsilon_p - j \frac{\sigma_p}{\omega} \\
\varepsilon_m^* = \varepsilon_m - j \frac{\sigma_m}{\omega}$$
(6)

where ε and σ represent permittivity and conductivity, respectively, and ω is the angular frequency of the applied signal. The frequency-dependent behavior of the Clausius-Mossotti factor means that it may have different magnitude and polarities depending on the frequency and accordingly a particle in the same medium may tolerate different forces and also both positive and nDEP depending on the frequency of the applied signal.

In the case that the sign of the Clausius-Mossotti factor is different in the two regimes, there is a frequency at which the real part of the Clausius-Mossotti factor is zero. At this frequency, which is called crossover frequency, a transition happens from pDEP to nDEP. The crossover frequency ω_0 can be calculated by [46]:

$$\omega_0 = \sqrt{\frac{(\sigma_m - \sigma_p)(\sigma_p + 2\sigma_m)}{(\varepsilon_p - \varepsilon_m)(\varepsilon_p + 2\varepsilon_m)}}$$
(7)

In this formula, to estimate the conductivity of the particles, the capillary electrophoresis technique can be utilized which is reported by White et al. [46].

Different studies [48, 49] reveal that at high frequencies $(\omega \tau \gg 1 \text{ where } \tau = (\varepsilon_p - \varepsilon_m)/(\sigma_p + 2\sigma_m)) \text{ permittivity of}$ the particle and suspending media determines the behavior of the system (dielectric regime), where the real part of the Clausius-Mossotti factor is estimated with $(\varepsilon_p - \varepsilon_m)/(\varepsilon_p +$ $2\varepsilon_m$). Accordingly, if the permittivity of the particle is larger than that of the medium, $Re[K(\omega)]$ is positive and the particle experiences pDEP force. In the case of $\varepsilon_p \gg \varepsilon_m$, $Re[K(\omega)]$ is at its maximum value of almost one, consequently, maximum force is applied to the particle in the same electric field intensity. In the case of $\varepsilon_p < \varepsilon_m$, $Re[K(\omega)]$ is negative and the particle experiences nDEP force. If $\varepsilon_p \ll \varepsilon_m$, $Re[K(\omega)]$ is at its minimum value of almost -0.5, and therefore, maximum nDEP force is applied to the particle in the same electric field intensity. On the other hand, at low frequencies ($\omega \tau \ll 1$) the conductivity of both particle and suspending media are the dominant factor (conductivity regime), where the real part of the Clausius-Mossotti factor is estimated with $(\sigma_n \sigma_m$)/($\sigma_p + 2\sigma_m$). Therefore, in the low frequency region, if

the conductivity of the particle is larger than that of the medium, $Re[K(\omega)]$ is positive and particle experiences pDEP force. In the case of $\sigma_p < \sigma_m$, $Re[K(\omega)]$ is negative and particle experiences nDEP force. Similar to the high frequency region, at low frequency regime $Re[K(\omega)]$ varies in the range of -0.5 ($\sigma_p \ll \sigma_m$) to 1 ($\sigma_p \gg \sigma_m$) based on the conductivity of both mediums. An interesting phenomenon based on the analysis is that the DEP force for pDEP is usually higher than that for nDEP. Since DEP force in different frequencies acts on different properties of particles, this can be utilized to efficiently distinguish among different materials such as cells [50-52].

III. DIELECTROPHORETIC METHODOLOGIES

As mentioned before, dielectrophoretic manipulation can be achieved if a nonuniform electric field is established at the designated location. There are two important methodologies to generate required nonuniformity in electric field distribution. These methods are categorized as either electrode-based DEP (eDEP) or insulator-based DEP (iDEP). Moreover, studies show that the time variability of electric fields (dynamic and static fields) is another parameter that should be considered to tune the performance of the device. Accordingly, the focus of this section is on the methods and considerations which is related to the electric field.

A. Electrode-based DEP

The eDEP relies on the presence of fabricated micro or nanoelectrodes which are in direct contact with manipulated materials and/or the suspending medium during the operation. Accordingly, electrode design is of important significance as geometry, arrangement, and material of the electrodes determines the functionality of the device in this structure. Electrode material should not chemically or electrochemically react with the sample in either the presence or absence of the electric field [53]. Fortunately, a wide variety of metals are suitable for most applications. Gold and platinum are the most common options since they are electrochemically stable and biocompatible. Indium tin oxide (ITO) is another choice if a transparent electrode is preferred. Since metallic electrodes are in direct contact with the sample, electrodes may electrochemically react with the sample during the experiment if the voltage level is high enough [54]. As an alternative, metallic electrodes can be replaced by doped silicon electrodes to decrease the electrochemical reaction effect [55, 56]. The thin native oxide layer formed on the electrodes produces a large interface capacitance. This decouples the strong electric field region from the electrode interface and, thereby effectively suppresses the electrochemical reactions [57]. With this strategy, it is possible to increase the voltage level to have a higher DEP force. Iliescu et al. presented a DEP device with highly doped silicon electrodes. They were able to increase the device voltage up to 25 V_{pp} to successfully move the cells toward the electrodes without damaging the device and materials. Although the silicon process is well established, the fabrication process for this type of DEP device is complex and expensive [55]. The fabrication process of carbon electrodes is

simpler and cheaper even for high aspect ratio structures [58]. Similar to doped silicon, carbon has higher electrochemical stability than frequently used metals in microfabrication techniques [59]. In fact, higher voltages can be applied to carbon electrodes without electrolyzing the sample. Since carbon provides outstanding biocompatibility, DEP devices based on carbon electrodes are frequently reported in biomedical applications [60-63]. As such, carbon electrodes can be a suitable alternative to doped silicon electrodes if the cost of the device is important. However, the resistivity of both carbon and doped silicon electrodes are much higher than the resistivity of metallic electrodes. Since DEP process does not require high current flowing electrodes, ohmic voltage drop on the carbon electrodes can be compensated by increasing the applied voltage level. Geometry and arrangement of electrodes are other important factors that should be suitable for generating the required nonuniformity in the electric field and satisfy the requirement for specific manipulation. For instance, electrode width and gap size in the trapping process should be in the range of the targeted material size. The electrodes pattern and their functionality are discussed in coming subsections.

Generally, the eDEP fabrication process is time-consuming and expensive [64], with specific challenges when dealing with nanomaterials since the device may require fabricating nanoelectrodes and nanogaps. Despite that, the eDEP approach is a convenient approach especially for the cases that requires performing characterization such as electrical and thermoelectric measurements on a single or a few objects. eDEP structure has the advantage of low voltage operation with higher DEP force. Based on the application, a variety of patterns are reported for electrodes such as electrode pair [65], interdigitated electrodes [66-69], polynomial electrodes (multiphase electrodes) [70-72], and 3D electrodes [73] which we will discuss in the following subsections.

1) Electrode pair configuration

The simplest and commonly used configuration to generate nonuniform electric field is the electrode pair configuration. This configuration consists of two micro or nanoelectrodes with a gap in between the tips, a typical device is shown in Fig. 2. A nonlinear electric field forms between the electrodes and its gradient depend on the gap geometry and applied potential. This structure is commonly used for the trapping process. Micro and nanostructures can be trapped and immobilized for future processing and characterization. A variety of particles such as biomaterials, carbon nanotubes, nanowires, and DNA have been trapped, immobilized, and characterized using electrode pair configuration [36, 74-76]. Castillo et al. reported an eDEP device with gold electrode pair consists of 1 μm gap in between electrodes. This device is used to manipulate, immobilize, and characterize self-assembled amyloid peptide nanotubes [6]. In another interesting work, Gong developed an attomolar protein detection device by trapping silicon nanowires in between Au/Ti electrodes [77]. In this research, they modify the nanowire after immobilization and make a nanowire field effect transistor (NWFET) which is used as a biosensor. In a recent study, we

introduced a device with a pair of nanoelectrodes on a sapphire substrate, shown in Fig. 2, is used to trap high impedance DNA origami structures. The device that consists of different DEP electrodes with gap sizes of 400, 600, and 800 nm was fabricated using conventional photolithography methods [65].

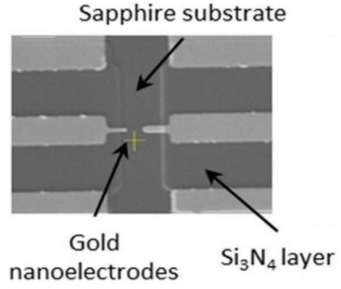
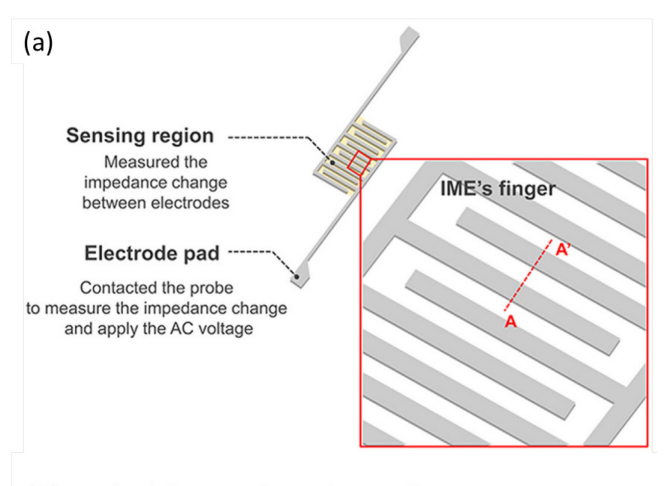


Fig. 2. SEM image of an eDEP device fabricated on a sapphire substrate. The device consists of a pair of gold nanoelectrodes (reprinted with permission from [53, 65]).

2) Interdigitated electrodes

Interdigitated electrodes are the second most commonly used configuration. The general shape of interdigitated electrodes is shown in Fig. 3(a). The fabrication process of these electrodes is well established since they have a variety of applications in MEMS and semiconductor technology. Interdigitated electrodes have received special attention since they can provide multiple trap regions as well as high throughput fabrication process [78, 79]. The field minima and maxima are distributed among the electrodes. A suitable design can offer both nDEP and pDEP behavior simultaneously. Thus, with multiple trap locations this device can provide a platform for both particle separation and filtering. For instance, in a specific case, larger and more polarizable materials can easily be trapped while small and less polarizable materials pass by the trap locations and leave the device. Because the device can work at a wide range of frequencies, it can be used to manipulate a variety of particles. In an interesting application, Kim et al. used this technique to improve the sensitivity and limit of detection of a biosensor [80] that detects biomolecules. They demonstrated an improvement in the binding efficiency of the antibody and target molecules as a result of increasing the concentration of the target molecules around the sensor using DEP. Recently, Challier et al. also reported an inkjet printing method for fabricating interdigitated electrodes [81]. The printed device could sort polystyrene particles, as well as separate planktonic species according to their composition.



(b) Applied the DEP force during the reaction

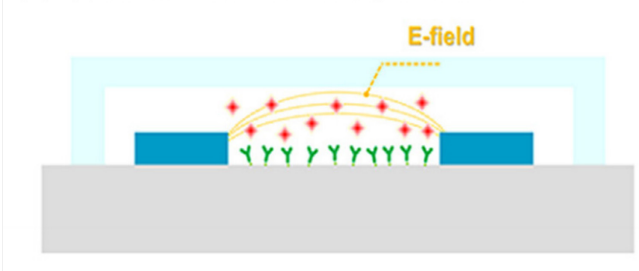
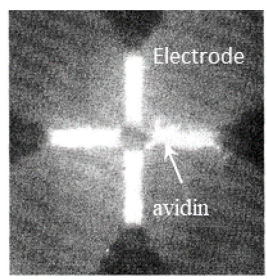


Fig. 3. schematic structure of (a) Interdigitated electrodes, and (b) the experimental process. DEP signal increases the concentration of target molecules around the sensing area to increase binding efficiency. (reprinted with permission from [80])

3) Polynomial electrodes

Polynomial, or multiphase, electrodes are composed of multiple planar electrodes with circular symmetry. The most frequently reported design contains four electrodes in a quadrupole configuration. This structure can be used for both trapping and electrorotation [70]. Moreover, the structure has multiple trap locations including at the center of the electrodes suitable for nDEP and the space between every two electrodes suitable for pDEP [82]. Bakewell et al. reported a quadrupole structure for selectively trapping biomacromolecules such as avidin using both pDEP and nDEP in different trap locations [83]. They demonstrated that avidin accumulated in the space between every two electrodes as a result of pDEP, as shown in Fig. 4 (left panel), at frequencies less than 9 MHz but avidin accumulated in the center of the electrode structure as a result of nDEP at higher frequencies, as shown in Fig. 4 (right panel). Since two or more signals can be applied simultaneously, the multiphase structure can provide more flexibility in terms of particle manipulation. In an interesting work, Zheng et al. used a quadrupole structure to flexibly move and position target cells [84]. The location of the cell is controlled by modulating phases and amplitudes of the two signals applied onto the quadrupole microelectrodes. These signals are applied diagonally and single cells can be controllably transferred in various directions on a chip.



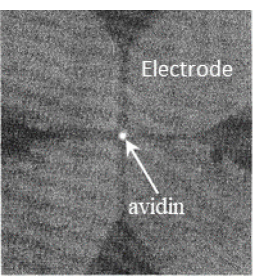


Fig. 4. quadrupole structure showing both pDEP (left panel) and nDEP (right panel). (reprinted with permission from [83]).

4) Three-dimensional electrodes

The main issue with the electrodes (planar electrodes or thin film electrodes) that we have discussed so far is that they suffer from low flow throughput. Although geometrical parameters of electrodes can be set for higher throughput [85], these electrodes generate an electric field gradient close to the surface of the electrodes and accordingly DEP force cannot be applied to the particles that are not in the close vicinity of the surface. This might be a problem for some applications such as particle separation when the sample volume is large. For instance, a study showed that the channel height in a microfluidic device with planar electrodes on the bottom and top of the channel cannot exceed 50 µm or else the DEP force will be insufficient to control particles in the middle of the channel [86]. To increase the throughput of the system or to manipulate large materials in the range of a few tens of micrometers such as cells, 3D metal electrodes should be used instead of the planar electrodes. With 3D electrodes, a DEP device can manipulate higher volumes than a structure with planar electrodes. Yamamoto et al. reported an interesting structure composed of three-dimensional nanoelectrodes arrays used for biomolecule study [73]. The fabricated nanoelectrodes (aluminum coated diamond-like carbon electrodes) with very sharp tips that are suitable to trap only one biomolecule on a single tip. By applying an appropriate signal, the device was able to trap target molecules on top of nanoelectrodes. Although the device showed a good performance for the immobilization and concentration of biomolecules at specific locations, the fabrication process required complex and expensive processes. Focused ion beam assisted chemical vapor deposition, plasma etching, and physical vapor deposition were required for the fabrication process [73]. Instead of using metals in the structure of the 3D electrodes, it is possible to use highly doped silicon. As mentioned before, silicon offers more electrochemical stability than commonly used metals, and accordingly, it is possible to apply higher voltages to increase the depth of electric field gradient and take advantage of well-established silicon technology in the fabrication process [57]. Similar to the previous example the main disadvantage of silicon technology is its complexity and expense.

Since 3D electrode structure has been proposed to increase material throughput, it is also recommended to have high aspect ratio electrodes. This electrode structure increases electrodes' effective surface area resulting in a higher allowable flow rate, and allows the entire height of the

microfluidic channel to be controlled. Silicon technology requires expensive fabrication processes such as deep reactive ion etching (DRIE) for high aspect ratio features. Carbon electrodes can solve this problem and it is possible to fabricate high aspect ratio 3D electrodes with simple fabrication processes such as pyrolysis. Moreover, carbon electrodes offer the advantages of doped silicon electrodes but with a cheaper fabrication process [58]. A typical set of 3D carbon electrodes used for dielectrophoresis and a cross sectional view of the whole device is shown in Fig. 5 [87]. Several experiments demonstrate the effectiveness of 3D carbon electrodes in material manipulation such as separation [87] and trapping [88]. Recently, 3D carbon-electrode dielectrophoresis (carbon-DEP) is reported as a separation tool for U937 monocytes and U937 monocyte-differentiated macrophages [89].

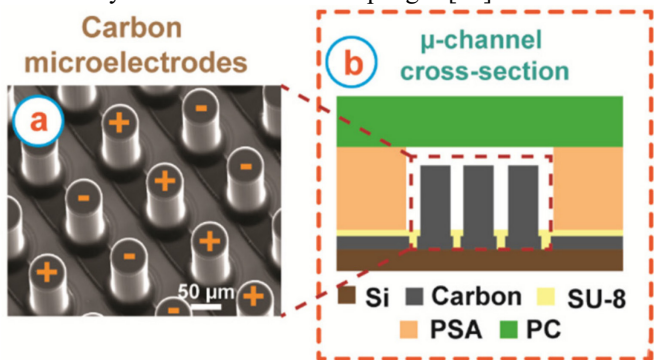
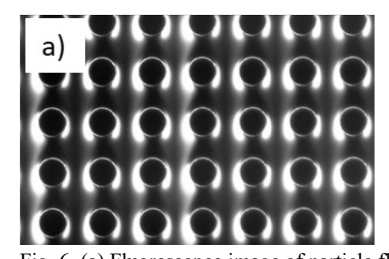


Fig. 5. (a) SEM image of the 3D carbon microelectrodes. (b) schematic structure of the cross section of the microchannel showing the different elements of the DEP device (reprinted with permission from [87]).

B. Insulator-based DEP

The working principle of the iDEP configuration is based on the arrangement of insulator materials in between the metallic electrodes. Generally, electrodes themselves are not responsible for generating nonuniformity in the electric field distribution but the arrangement of insulators with different permittivity, shapes, and sizes in between the metallic electrodes changes the electric field distribution and produces the desired field gradient [90]. Generally, the electric field gradient is maximized in close proximity to high permittivity materials and minimized at the voids between insulators. The size of the insulators is extremely important to generate the desired field profiles as small size particles generate higher field gradients [48, 91]. In these cases electrodes are not in direct contact with the solution and high intensity or low intensity regions of the electric field are shaped between the incorporated insulators. Accordingly, this configuration is called electrodeless, contactless, or insulator-based DEP. Generally, insulator-based DEP has the advantage of only requiring simple and inexpensive fabrication processes since the shape and size of the metallic electrodes are not critical. iDEP devices can be fabricated on polymeric substrates using mass fabrication methods such as injection molding or hot embossing techniques [90, 92, 93]. The number, size, and shape of the insulating objects is determined based on the manipulation function and the physical properties of the manipulated materials [94-98]. Manipulating a variety of materials is reported in the literature using iDEP devices ranging from DNA to biological cells and other rigid materials [99-101]. The iDEP shows higher efficiency specifically for biological samples since materials such as cells are not in direct contact with energized electrodes, as such, materials are not damaged.

To the best of our knowledge, Masuda et al. reported the first iDEP device for cell fusion in 1989 [99]. They guided cells toward a small opening made at the center of an insulating barrier and trapped cells in that location, then the cell infusion process was performed at that location. This work motivated other researchers to develop more efficient structures and improve the performance of the iDEP method. Cummings et al. reported structures composed of an array of insulating rods filled in a microfluidic system for concentration, filtration, and separation applications [101]. They used this device to manipulate fluorescent particles with a diameter of ~200 nm. Fig. 6(a) shows that the particles are trapped in the areas around the rods where electric field intensity is high. In another study, Chou et al. trapped single and double-stranded DNA using iDEP technique. The device contained array of trapezoidal insulating posts made of crystalline quartz with pitch of 1 µm. The required electric field intensity was generated by applying an AC signal with an amplitude of 1kV and frequency in the range of 200 Hz to 1 kHz [102]. Fig. 6 (b) shows that the 368-bp stranded DNAs are successfully trapped. This structure is frequently used to manipulated other materials such as DNA [103], proteins [104-107], mitochondria [108, 109], and carbon nanotubes [110]. The voltage required for operating iDEP is very high and this is considered as a drawback of the iDEP method since it can increase the temperature of the device and materials due to Joule heating.



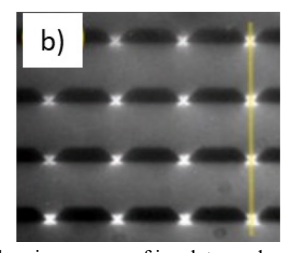


Fig. 6. (a) Fluorescence image of particle flow in an array of insulator rods. This image shows the trapped particles (200 nm fluorescent spheres) in high intensity region of the electric field (reprinted with permission from [101]). (b) Optical micrographs of DEP trapping with an applied potential of 1 kV (reprinted with permission from [102]).

Joule heating is an unwanted problem in most DEP devices. Joule heating is the result of the electric current flowing through the materials involved. The electrical conductivity of the medium in between the electrodes is an important factor that increases the joule heating [111]. Although the electrodes in eDEP configuration are in direct contact with the solution, iDEP devices suffer more since they generally demand higher voltage levels to operate. Joule heating is an undesirable effect since it can adversely affect the performance of the device by damaging particles, releasing the trapped materials, or changing the properties of the suspending media [112-115].

Joule heating can increase the Brownian motion of the particles, induce fluid motion, and change the DEP force. These effects decrease the reliability of the DEP process [113, 116-124]. As such, much work has focused on decreasing the voltage required to drive an iDEP device. Generally, low voltages have the advantage of lower Joule heating effects and releases more applications for iDEP specifically in biology [117]. In order to decrease the applied voltage level of iDEP devices a few strategies have been developed. Embedded passivated-electrode iDEP (EπDEP) structures [125, 126], three-dimensional iDEP (3DiDEP) [117, 127], conductivity gradient-based DEP [128] are three examples of efficient structures that demand lower applied potentials. In the $E\pi DEP$ structure, electrodes are located in close proximity while covered with an insulating layer. The operating principle is similar to iDEP structures since materials are not in direct contact with electrodes. High intensity electric fields can be generated with much lower potential in the range of tens of volts. However, electrode fabrication is not simple as normal iDEP structures. 3DiDEP structure combines the advantages of 3D electrodes, iDEP, and eDEP configurations with the goal of high throughput manipulation at lower potential [125]. The fabrication of a three-dimensional structure with high aspect ratios is discussed in section 5. A 3DiDEP structure allows trapping manipulated objects with lower applied potential. For instance, 10 µm beads were successfully trapped in a 1 cm long channel with an applied potential of 10 V, and E.coli cells were trapped at an electric field of 50 V/cm [117]. In another study, Diana et al. presented a device with a 3D structure fabricated on a silicon wafer using reactive ion etching, as shown in Fig. 7(a) and (b) [125]. The device can trap objects in the area between the microposts, as shown in Fig. 7 (c), while fluid flows in the microfluidic channel. The presented device could selectively trap 90% of the live bacteria at frequencies ranging from 30 to 60 kHz at 400 Vpp while most of the dead bacteria escaped. As shown in this example, 3DiDEP structures can be arranged to fabricate high through put filters. In fact, in this structure, suspended target particles are continuously immobilized in multiple trap locations if the DEP force is stronger than drag force applied by liquid flow. As a filter application, iDEP processes have received special attention in biology to filter out specific cells. One advantage of the DEP filter is that filter cleaning process can be done by simply releasing the trapped particles when the applied potential is removed [111, 129-131]. In conductivity gradient-based DEP, an ionic liquid is used to form the electrodes in a microfluidic chip. The immiscibility nature of the selected ionic solution in the DEP liquid provides a stable interface in the microfluidic channel. The absence of an insulation layer between the liquid electrodes and DEP buffer improves the coupling efficiency and makes full use of the electric potential applied into the main channel to generate a strong enough electric field gradient. In this structure, two DEP buffer is used and the gradient of the conductivity of DEP buffers is responsible for inducing the gradient of the electric field. Specifically, the nonuniform electric field is generated by using two types of DEP buffers with different

conductivities. This method showed an efficient DEP separation of cells and particles in the device [128].

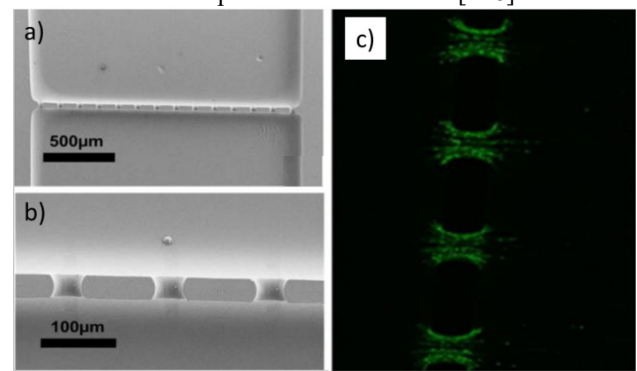


Fig. 7. (a) SEM image and (b) magnified image of a iDEP device with 3D microposts. (c) Low voltage operation of the device showing that materials are concentrated at the microposts (reprinted with permission from [125]).

There are other iDEP structures reported for specific purposes such as a nanopipette system for trapping short length DNA and single-nucleotide triphosphate particles [35], porous membranes for trapping a wide array of particles, ranging from biomolecules to cells [129-134].

C. AC or DC Electric field

As discussed, Joule heating is an unwanted phenomenon in DEP process and the trend is to find methods to decrease the generated heat during the device operation. One possible method is to design a suitable structure operating with lower voltage levels (discussed before) and using a substrate with high thermal conductivity such as silicon [124] to dissipate generated heat, thus allowing the device to operate at lower temperatures. The other method involves taking advantage of the AC field.

In general the use of a high frequency AC signal (greater than 100 kHz) for DEP purposes has some advantage over DC or low frequency DEP. First, electrochemical reactions decrease even if the potential level is high enough to initiate the reaction [93]. This reaction can occur between each part of the device such as electrodes, substrates, insulators, and solution. The reaction often generates bubbles. Second, experimental and simulation results confirm that DC voltage can produce significantly more Joule heat than an AC voltage [94, 100]. Third, the AC field prevents electrophoretic movement of statically charged materials such as cell membranes [135]. All these can be achieved at the cost of the insulation problem. Thin insulation layers between the electrodes and substrate or other parts of the device cannot efficiently block a high frequency AC signal, and this can adversely affect the functionality of the device by decreasing the electric field gradient and increasing the leakage current. Moreover, the leakage current can interfere with the monitoring circuit, affect its operation, and decrease its sensitivity. This is a common problem for the devices made from silicon wafers since silicon is not an insulator. Even insulating silicon nitride (Si₃N₄) or silicon dioxide (SiO₂) layers grown on the silicon (Si) wafer makes a low impedance path to the underlying Si material at high frequencies (> 1

MHz). Since silicon is not a very high impedance material, DEP devices on these types of wafers suffer when attempting to detect high impedance materials such as DNA origamis. Sapphire wafers are reported as an alternative substrate for silicon wafers for dealing with very high impedance materials; however, its surface properties can become another challenge in immobilizing the trapped particle. Different studies show that a suitable surface preparation such as Silanization can alleviate this problem for a range of particles [65, 136-138].

Although the AC field has numerous advantages over the DC field, the DC signal can be successfully applied to low voltage iDEP configuration since the insulating layer can prevent the occurrence of electrochemical reactions [139] and decrease the leakage current. One other possible method to decrease the DC voltage level is to apply a DC-biased AC signal. DC-biased AC electric fields can improve the functionality of iDEP devices [140-143]. In a study, Zellner et al. show that the use of DC-biased AC fields improved selectivity for trapping bacteria in 3DiDEP microfluidic devices over DC operated iDEP devices. For example, the separation of *Escherichia coli* from 1 µm beads and the selective trapping of live *Staphylococcus aureus* cells from dead cells are reported [140].

IV. DIELECTROPHORETIC MANIPULATION

DEP forces can be used to trap, separate, and transport a variety of materials. The focus of this section is the application, challenges, and some examples of DEP devices in micro and nanomaterial manipulation.

A. Trapping

One of the most important applications of the DEP technique is trapping. As discussed in section 2, the DEP force is related to the gradient of the electric field. This force can act on an object and moves it toward or away from the field gradient. Accordingly, the trapping process is successful if the electric field gradient provides stronger force than the surrounding forces such as thermal force to the particles and guides it to the specific location with net-zero DEP force. In the literature, both nDEP and pDEP forces are employed to trap materials. Specifically, for the eDEP configuration, the size of the electrodes and the gap between them may need to be in the same range as the object under investigation, otherwise objects can accumulate instead of trapping only individual or a few oriented particles. Accordingly, the trapping nanomaterials requires the fabrication of nanogaps and nanoelectrodes. Nanogaps and nanoelectrodes are highly sensitive to the applied voltage and electrostatic discharge since even low voltages can generate extremely high-intensity electric fields in the gap and around the sharp electrodes. This electric field may destroy the device and material. For instance, the formation of nano-canyons with depths of 10 to 40 nm on a SiO₂ substrate in between the nanoelectrodes is reported during the trapping procedure while the applied voltage level to the electrodes is about 5 V_{PP} [34]. In this case, 5 V_{PP} generates an ultra-high intensity electric field in an 80 nm gap region and around the sharp edges of the electrodes.

This may locally destroy the silicon dioxide substrate and the electrodes. This issue makes it difficult to deal with nanomaterials. In addition, the fabrication process for nanoelectrodes and nanogaps requires a sophisticated processes that are expensive, complex, and low throughput. Electron beam lithography, a commonly used fabrication technique for patterning nanostructures, is frequently applied to design DEP devices for trapping nanoparticles [34, 144].

Even though material trapping has been successfully demonstrated in a variety of conditions, it remains challenging to confine only a single object. Since the presence of a nonuniform electric field in between electrodes continuously attracts polarizable objects to the trap location, a mechanism is required to control the trapping process, detect the presence of the material, and prevent particle accumulation in between the electrodes. In some studies, this process is calibrated based on the properties of the applied signal. The trap mechanism is adjusted based on the applied voltage level, the frequency of the signal, the solution concentration, and the duration of the process [37, 65, 68, 145]. Since there is no feedback mechanism in this procedure, the system is highly sensitive to the mentioned parameters and other unwanted environmental parameters such as temperature and pressure changes. Accordingly, this process is typically low yield. With a gap the size of the target material, one can slightly increase the efficiency of the device since it is possible to apply the signal more than the normal time without having significant aggregation. Kuzyk et al. proposed a DEP device that controls the trap mechanism by tuning the buffer concentration, applied voltage levels, and frequency [146]. They reported 10% efficiency in precisely trapping the origamis in between the electrodes. In other research, Shen et al. reported a yield of higher than 50% for anchoring DNA origamis to gold nanoelectrodes [34]. Although this method shows a moderate success rate, it is highly sensitive to the experimental conditions and a slight change requires additional calibration. Since there are inevitable small changes in the electrode shapes between DEP devices or the solution concentration of different samples, trapping based on the previous calibration results in low yield. The yield is even lower if either the device fabrication or sample preparation processes are modified. However, a few promising studies have shown that monitoring the trap location can significantly increase the yield of the process and decrease the sensitivity of the process to the mentioned parameters [147, 148]. The monitoring is usually based on impedance measurements. Having a monitoring system can provide increased tolerance to changes in the fabrication process and remove the requirement of fabricating the electrodes with precisely the same parameters. This decreases the cost of fabrication especially when dealing with nanomaterials. In fact, the monitoring system can often be used to stop the process before aggregation occurs. However, the monitoring system can be challenging to implement when dealing with high impedance materials such as long DNA origamis. We reported a method to detect the presence of high impedance one dimensional DNA origamis by a high sensitivity capacitance measurement circuit [65].

This specific electronic circuit is designed for both trapping and monitoring. The presence of this electronic circuit alleviates the requirement of having narrow electrodes. Although the width of DNA origamis is in the range of 10 nm (cross-section area of 10 nm×10 nm), electrodes with 400 and 600 nm widths are suitable for the trapping procedure without having significant aggregation problems. This circuit, which is a high sensitivity capacitance measurement, detects the presence of nanomaterials in the trap location, therefore the trapping process can be stopped at an appropriate time. There was no destruction of electrodes or gap, and this might be attributed to the relatively wide electrodes and use of sapphire substrates.

Some structures offer multiple trap locations. The quadrupole structure discussed above is a famous example structure. Different reports illustrate that the nDEP force can trap the particle in the center of the structure and pDEP force can trap the particles in between each electrode pair. nDEP can move the objects of interest toward the center of the electrodes in a quadrupole structure [82]. Even a successful demonstration for trapping nanoparticles as small as 14 nm has been reported [149]. Huges and Morgan demonstrated the trapping of a latex nanosphere in a center of a quadrupole structure [150]. Similarly, interdigitated electrodes can show the same behavior but provide multiple trap locations. In a study, Alexandrium minutum (AM) and Prorocentium micans (PM) are selectively trapped in specific locations based on the frequency response. AM cells have a frequency feature with an approximate crossover frequency of 8 kHz. Above this frequency, pDEP force applies to AM cells and they experience nDEP for lower frequencies. PM cells show pDEP behavior for the working frequency range. At high frequencies, both AM and PM cells accumulate in pDEP zones, shown in Fig. 8(a) and (b), whereas at 5 kHz, only AM cells accumulate in nDEP areas (see Fig. 8(c)) [81]. In another study, a trapping device based on an electrode array is reported. This device trapped and harvests microalgaes with an efficiency of 96.18% [130].

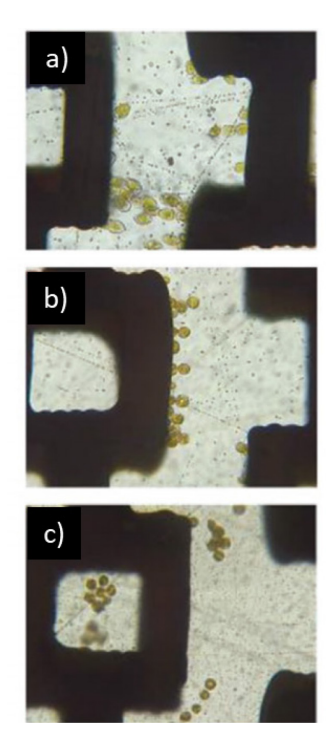


Fig. 8. a) PM trapped in pDEP area at 10 MHz, b) AM trapped in pDEP area at 10 MHz, and (c) AM trapped in nDEP area at 5 kHz (reprinted with permission from [81]).

For success, the DEP force must be strong enough to adsorb the material to the designated trap location and return it to the location if the material deviates as a result of external forces such as vibration and fluid flow as well as temperature-driven forces such as Brownian motion. The presented devices move the particle toward the trap location, however, gravity is responsible to hold large particles such as cells on the surface [149, 150]. Most micro and nanomaterials and even objects with near neutral buoyancy can easily escape from the trap location as a result of small turbulence. 3D structures [151, 152] can improve the performance of the device in confining particles more strongly.

Since eDEP structures provide post-processing capabilities after the trapping process to measure properties of the materials, they are often used for the trap procedure. However, analysis of some samples such as cells is done in a solution phase in a micro-reaction chamber. Also accessing the single cells data enriches the knowledge of sustaining challenges in molecular biology, cancer diagnostics, pathology, and therapy [153, 154]. That being said, trapping an individual cell in an iDEP device provides a suitable platform for studying important features of that specific sample [155]. Bhattacharya et al. reported an iDEP device in a microfluidic chamber that traps individual cells using insulating posts integrated at microchannel intersections, as shown in Fig. 9 [153]. They could successfully trap polystyrene particles of 10 mm diameter and a single MCF-7 breast cancer cell.

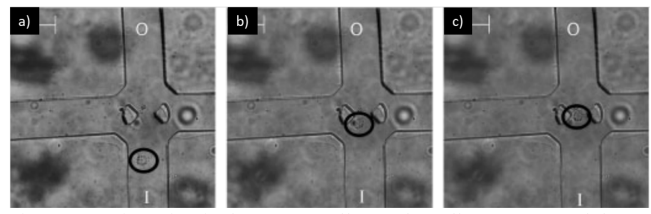


Fig. 9. Trapping of a single MCF-7 cell. (a) The cell moves toward the tap location. (b) The cell is directed toward the tips of the trap location. (c) The cell is trapped by iDEP force [153].

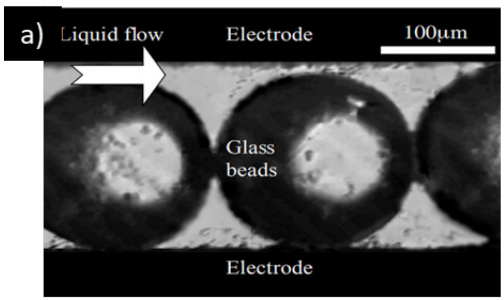
Additionally, after a successful trap, another challenge in the dielectrophoretic trap is immobilizing the particle in trap location for future studies such as I-V and C-V measurements. In order to measure the properties of an individual or a group of particles as well as the environmental effect on the particle properties, we need to dump the solution or exchange the environmental condition without moving or detaching the trapped materials. This requires a firm connection of the particle to substrate and electrodes. Surface chemistry plays an important role in immobilizing materials in the trap location even after removing the trap signal. This is usually accomplished by altering the surface properties and attaching anchoring groups to the trap location and/or manipulated materials. The type of particle, anchoring groups as well as substrate itself play an important role in reliable and repeatable measurements. For instance, DNA origamis can perfectly attach to the hydrophilic SiO₂ surface. Accordingly, different studies show that if the electrodes are made on the SiO₂ substrate, DNA origamis are perfectly immobilized after trap, and changing the environmental condition does not move the origamis. However, some substrates may not be suitable for immobilizing trapped materials. In such a case, the surface properties of the chip should be altered by using specific chemicals. For instance, the single crystalline sapphire (0001) surface encompasses hydrophobic regions inside hydrophilic areas [138]. Therefore, materials such as DNA origamis does not firmly attach to the surface of sapphire, and they may displace during or after the trap procedure. Accordingly, the sapphire surface are usually functionalized using 3-Aminopropyl triethoxysilane (APTES) for covalently binding biomaterials to inorganic surfaces [136]. Ghomian et al. carried out a liquid phase deposition of APTES on the sapphire substrate to enhance the adhesion of DNA origamis to the surface [65]. Moreover, anchoring micro and nanomaterials with some functional groups such as thiols and amines increases the attachment force of materials to the electrodes or substrate. In recent work, we modified DNA origamis with thiols on both ends to firmly attach them to the gold nanoelectrodes of the device. In another study, O2 plasma is applied to the quartz substrate to render the surface hydrophilicity for increasing the surface force in holding trapped nanowires and prevents displacement as a result of fluidic flow or other external forces [15].

B. Particle separation

Physical filtration is a traditional method to separate particles. However, pore clogging is a common problem that

adversely affects the operation and makes it impossible to use the device. More notably, if the process comes to separate same size materials or deal with very small materials such as nanoparticles, physical filtration fails. DEP is an excellent alternative tool for particle separation. The process works because the DEP force depends on the size, permittivity, conductivity of the particle, and the electric field gradient (DEP force on materials is explained in section 2). Since the electric properties of materials vary based on the frequency of the applied signal, the voltage amplitude and frequency of the applied signal may be tailored in a way to apply enough different forces to the different particles. This variation in the applied force along with the device structure can provide a suitable medium for particle separation.

One of the simplest structures is based on the iDEP configuration. In this structure, a fluidic channel is filled with insulators. The insulators could be in different shapes such as rods, spheres, textiles, etc. The microfluidic channel is equipped with pair of electrodes. As discussed in chapter 3, the insulators are responsible for making nonuniformity in the applied electric field [48, 91]. This approach can be used as a filter to separate different particles in a solution by trapping specific materials. Zhou et al. used 200 µm glass beads to fabricate a iDEP device to separate biological cells in water [156]. Fig. 10 shows that after applying the voltage (50 V_{pp}, 100 kHz) yeast cells are trapped in the field maxim in between glass beads. Since the insulators are readily available at a cheap price, the overall fabrication process is cheap and simple.



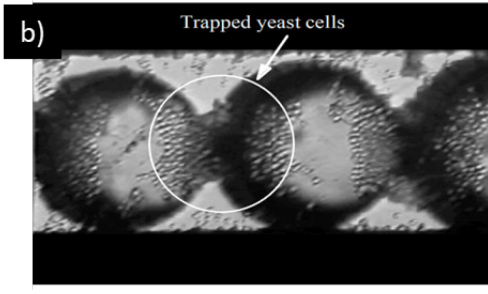


Fig. 10. an iDEP structure with glass beads in a microfluidic channel. (a) no yeast cell observation around the glass beads before applying the electric field. (b) applying the voltage (50 Vpp, 100 kHz) attracting and trapping yeast beads in the electric field maxima around the beads (reprinted with permission from [156]).

Interdigitated electrodes are another option for particle separation because they offer multiple trap locations for both nDEP and pDEP. One sophisticated mechanism involves taking advantage of the transition from nDEP to pDEP or vice

versa. In this method, one material experiences one type of DEP force (for example pDEP), and the other experiences the other type of DEP force (in this case nDEP). This method has been used in different studies to separate yeast cells [66], biological cells [157], and submicron particles [41] using interdigitated electrodes. Markx et al. separated viable and non-viable yeast cells in high electric field gradient and low electric field gradient regions respectively as shown in Fig. 11 [158]. The viable and non-viable yeast cells show different DEP behavior at 10 MHz, accordingly, they could separate them by applying 10 MHz electric field. At a low frequency of 10 kHz, both cells show pDEP behavior.

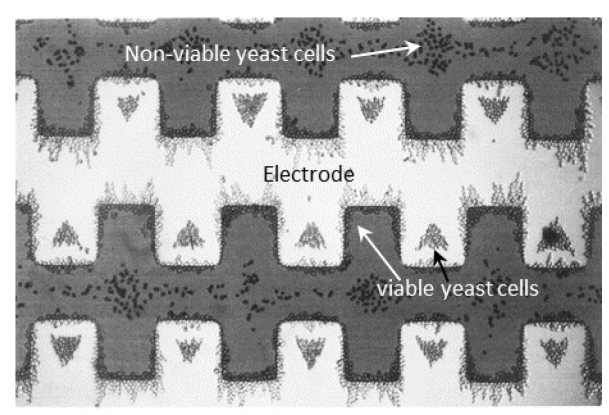


Fig. 11. Dielectrophoretic separation of viable and non-viable yeast cells using interdigitated electrodes. The viable yeast cells collect on electric field maxima around the edges of and in pearl chains between the electrodes, whilst the non-viable cells collect on electric field minima in between the electrodes in diamond-shaped formations (reprinted with permission from [158]).

Since the size of the particle affects the magnitude of the DEP force, some studies take the advantage of this property to separate large particles such as macromolecules from small objects such as DNA and viruses. Morgan et al. presented an electrode array DEP device fabricated using direct write electron beam lithography to separate different types of submicron latex spheres [41]. Particle separation is achieved if there is a regulated liquid flow around the DEP device to remove the free particle or particles trapped at field minima but leaving the trapped particles at field maxima (for pDEP case). Finally, the trapped particles was collected by turning off the applied signal and rinsing the electrode with the appropriate solution [159].

In an interesting study, a DEP device, shown in Fig. 12(a), is composed of two sets of electrodes on top and bottom of a microfluidic channel. This shape provides suitable trap places for both pDEP and nDEP. This device was used to separate planktonic species, Alexandrium minutum (AM) versus Prorocentrum micans (PM), according to their composition response to the frequency of the electric field. Moreover, the device was able to sort polystyrene particles as a function of their size, with diameters ranging from 0.5 to 5 μ m. This work demonstrates a device that can separate the components of samples at flow rates up to 150 μ L/min. In this process, a blend of AM and PM is introduced to the chip. At the frequency of 12.5 MHz, both AM and PM cells are accumulated in the first trap areas as a result of pDEP force,

shown in Fig. 12(b). Then, by switching the frequency to 5kHz, AM cells show nDEP behavior while AM cells have the same pDEP behavior. Accordingly, the AM cells are released from the high electric field gradient areas of electrodes while PM cells remain trapped, shown in Fig. 12(c). AM cells are pushed away from the first trap region by the fluidic flow and leave PM cells in the first trap area, shown in Fig. 12(d). Since the next trap area is designed for the nDEP behavior, AM cells are trapped in that area, as shown in Fig. 12(e). This demonstration shows that a suitable electrode configuration in combination with frequency dependent DEP force can be used to separate materials. Since inkjet printing is not suitable for fabricating electrodes with a small gap, the main challenge of this device is manipulating materials less than 0.5 µm since a stronger electric field is required for small objects and that demands close separation between electrodes [81].

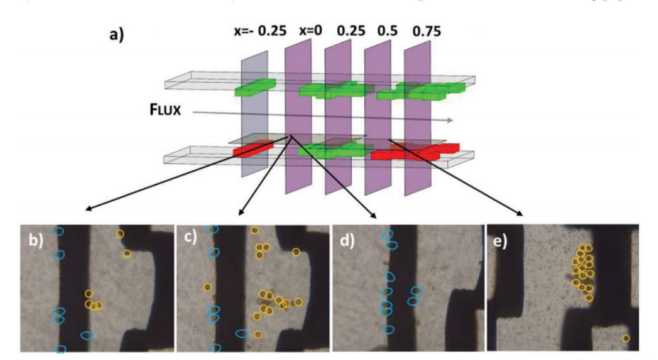


Fig. 12. (a) The schematic structure of the SEP device accommodated both nDEP and pDEP trap area. The printed electrodes are places on the top and bottom of the microfluidic channel. (b) both AM and PM cells are trapped with 12.5 MHz signal. (c) AM cells are released when the signal is switched to 5 kHz and (d) PM cells remain trapped. (e) AM cells trapped in the field minima at the second trap location as a result of nDEP force (reprinted with permission from [81]).

Moreover, variation in a particle's electric properties impacts the magnitude of the DEP force resulting in different behavior of the particle under the test. This provides a good platform to separate the same particles with different quality. This is suitable for a variety of purposes such as biomedical applications [52, 160] for detecting aged cells [161], cancer cells [162], separating monocytes from cancer cell [163], and differentiating mesenchymal stem cells [164]. A study shows that DEP force that acts differently on a Chinese hamster ovary (CHO) cells subjected to thermal stress and a normal CHO cell separate them and even can detect and separate the recovered cells [165]. An additional exciting study shows that it is possible to identify and separate bovine red blood cells (bRBCs) of varying starvation ages. The device works based on the fact that after glutaraldehyde fixation reactions the crossover frequency can vary as a function of the age of bRBCs. In particular, a bRBC has two crossover frequencies. The high crossover is dominated by internal cell parameters, such as cytoplasmic conductivity and permittivity, and is normally above 10 MHz in low conductivity media. The low crossover frequency is sensitive to changes in the cell membrane permittivity. Cross-linking by glutaraldehyde decreases the relative permittivity of the cell membrane from

10.5 to 3.8 depending on the age of the cell. The author adjusts the low crossover frequency to separate bRBC cells based on age [166]. Fig. 13(a) shows a quadrupole structure used for the separation experiment. As we discussed in section 3, quadrupole structure offers trap sites for both nDEP (center of the structure) and pDEP (area between every two electrodes) methods. In the experiment, if the frequency does not choose correctly all RBCs can show pDEP and be trapped in the area between the electrodes and electrode edges, as shown in Fig. 13(b), or they may show nDEP and be trapped in the center of the structure, as shown in Fig. 13(c). the authors demonstrate that at the frequency of 1.5 MHz it is possible to separate 4 weeks old cells (gathered in the center of the device) from 1 week old cells (trapped in the edge of the electrodes).

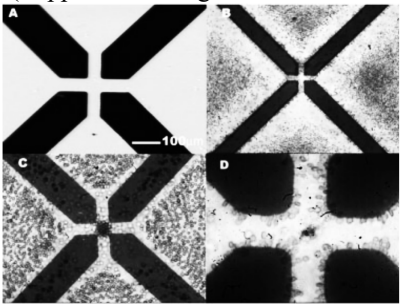


Fig. 13. (a) quadrupole electrode array used for bRBCs separation. (b) pDEP behavior observation of bRBCs. (c) nDEP behavior observation of bRBCs. (d) separation of 4 weeks old cells (gathered in the center of the device) from 1 week old cells (trapped in the edge of the electrodes) (reprinted with permission from [166]).

Hajari et al. presented a simple but useful structure that separates and sorts particles based on their sizes. This structure, which is consists of two tilted electrodes in a microfluidic channel, works based on the fact that the DEP force is related to the size and electric field gradient. Fig. 14(a) shows the two tilted electrodes and the fluid direction is from left to right. The DEP force is maximum at the location that the distance of two electrodes is minimum and the force decreases as the electrodes are separated. Moreover, as discussed in section 2, large particles experience higher DEP force. That being said, large particles cannot pass the electrodes at the location of the highest gradient (where two electrodes are in closest proximity) and a fluidic flow moves them along the electrodes toward the region of the low field gradient. At a specific point, which is called the release point, DEP force is not strong enough to keep the particle on the electrode, and therefore the flow of the fluid releases it. This release point depends on the size of the particle (assuming particles are made of the same materials). As shown in Fig. 14(a), as the particle gets bigger in the size, the release point moves further toward the low gradient region [167]. Fig. 14(b) and (c) show the experimental and simulation results of a device acting on polystyrene beads of a specific size. Both confirm that there is a specific release point for the particle having the same size.

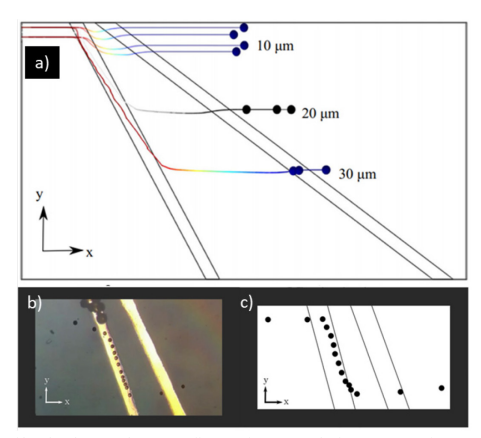


Fig. 14. Tilted electrodes configuration used for separation and sorting particles based on their size. (a) simulation results confirming the functionality of the device. larger particles experienced higher DEP force and they are released at the region with a lower field gradient. (b) experimental and (c) simulation demonstration showing particles with similar diameters moving along the electrodes and freed at the released point (reprinted with permission from [167]).

Microencapsulation of cells in hydrogels has a variety of applications in bioscience and bioengineering. However, the extraction of microcapsules from the oil phase in microfluidic systems is a challenging task. He group presented DEP for the separation of cell-laden hydrogel microcapsules from oil emulsion into an aqueous solution [168, 169]. In an interesting design, the device, which is based on the liquid electrodes, shows a reliable operation for redirecting hydrogel microcapsules toward the aqueous phase regardless of their mechanical strength [168]. Moreover, a study shows that the presence of DEP force can improve the efficiency and throughput of the circulating tumor cells (CTC) separation and detection. In this study, the device consists of two capture and flow zones. DEP force is employed to extract cells from the flow zone to the capture zone where the flow rate is low for accurate CTC detection [170]. Recently, machine learning methods are employed to improve the performance of the DEP devices. The application of the deep learning image analysis technique realized a real time labelfree detection and selective extraction of cell-laden hydrogel microcapsules [171]. Also, the Fuzzy logic method is utilized to optimize the design of a system for efficient separation of platelets from Red Blood Cells [172].

C. Particle Transportation

Transportation of micro and nanomaterials such as biological samples has played an important function in a variety of fields such as nanoscience, sensors, drug discovery, genetic sequencing, and cell sorting [173, 174]. Transporting targeted materials toward a specific location increases the concentration leading to accurate and efficient detection of that specific material [175]. Since DEP can apply force to the materials, this force can be used to guide materials on a predefined path (transportation) or toward a specific location (concentration). The working principle is a sequence of trapping and releasing in a specific pattern. To generate the pattern, a specific design for the size, geometry, and

arrangement of electrodes as well as the sequence and specification of the applied signal is required. Zaman et al. reported an array of microelectrodes to transport colloidal microparticles. They achieved this goal by applying AC voltage in a regular sequence to microelectrodes. This moves colloidal microparticles along the electrodes in the same pattern of the voltage sequence [176], manipulating substantial sets of small objects demands sophisticated technology [177]. In particular, the device should be able to have more selective transport on an arbitrary path for selected particles. In a study, Hunt et al. presented a creative method that is able to simultaneously and independently trap and transport thousands of dielectric materials along a particular path [178]. This device, shown in Fig. 15, combined integrated circuit (the chip consists of an array of 128×256 pixels, $11 \times 11 \mu m^2$ in size, controlled by built-in SRAM memory), microfluidic, and DEP technology. Although this is a complex and expensive device, but it opens a horizon to precisely move and locate the micro and nanoparticles for specific applications such as individual living biological cells and chemical droplets.

The manipulation of liquid droplets has been widely studied for a variety of applications such as biological [179], and thermal applications electrical, optical, [180]. Accordingly, droplet transportation has received special research attention. DEP force can be utilized to move the droplets in a specific direction. The presented device was able to precisely transport a water droplet towards a specific location, split a water droplet, and merge them, as shown in Fig. 15(d). However simple and cheap structures are introduced for this purpose. An array of electrodes [180] and an array of interdigitated electrodes [181] are two simple structures reported for droplet transport. Recently, the sequentially addressable dielectrophoretic array (SADA) sorter is introduced to combine the advantages of high-throughput single-cell sorting with those of large-droplet microfluidics to improve the throughput of droplet sorting techniques [182]. Another interesting structure is reported by Frozanpoor et al. which is an interdigitated electrode pad with a variable gap, as shown in Fig. 16(a) [183]. A droplet moves toward a high electric field gradient (or low electric field gradient based on the DEP operation) when a DC or AC signal is applied. Fig. 16(b) shows that set of the electrode pads are arranged in a matrix format. Signal management system connect to this arrangement provides accurate control on the location of the droplet in a one-dimensional movement. They show that with different arrangements if electrodes radial-symmetric droplet motion (Fig. 16(c)) and bilateral-symmetric droplet motion (Fig. 16(d)) are achievable.

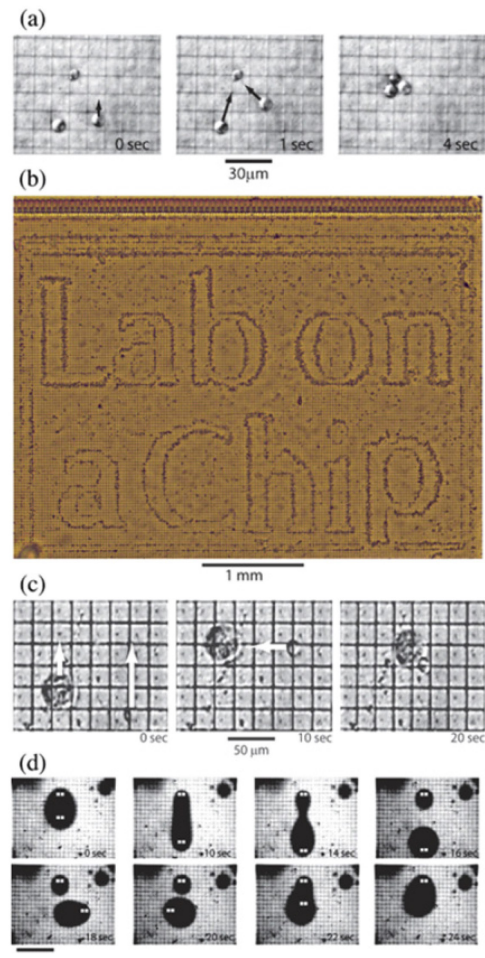


Fig. 15. (a) Transportation of two yeast cells toward the third one in 4 seconds. (b) Thousands of yeast cells patterned by DEP force to spell out "Lab on a Chip". (c) Independent transportation of yeast and rat alveolar macrophages manipulated with DEP. (d) Splitting, moving, and combining water drops in oil with DEP (reprinted with permission from [178]).

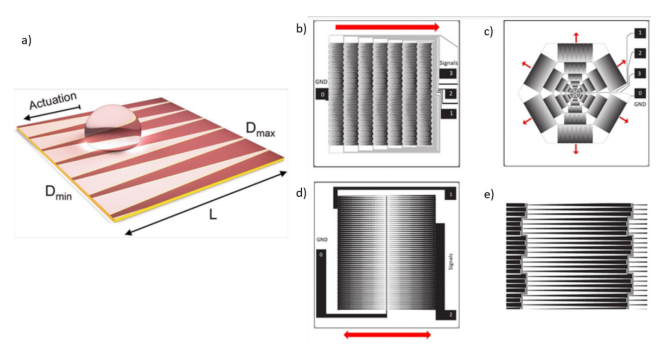


Fig. 16. (a) Interdigitated electrode pad with a variable gap. Arrangement of the electrode pads in a matrix format for controlling the position of the droplet in (b) linear, (c) radial, and (d) bilateral movements. (e) close view showing the overlapped region between two electrode pads (reprinted with permission from [183], further permissions related to the material excerpted should be directed to the ACS,

https://pubs.acs.org/doi/10.1021/acs.langmuir.1c00329,).

Another sophisticated method of transportation is changing the electric field pattern formed between the electrodes. If the electric field distribution form as a result of the interference of multiple electric fields, a change in magnitude and phase of the constituent components can change the overall field distribution resulting in different gradient patterns and different locations for minima and maxima in the electric field. This method required multiple electrodes and signals. Although this method should accompany by a signal processing module, provides a flexible and useful device for research activities specifically in biology. Zheng et al. design a method that is able to transport a cell on a chip by modulating phases and amplitudes of electrical signals applied to microelectrodes [84]. In this design, they used a quadrupole structure and applied two signals to form the final distribution of the electric field. Fig. 17 represents the simulation and experimental results. They could successfully transport a cell in the direction and location of interest by modulating the phase and amplitude of the DEP signals.

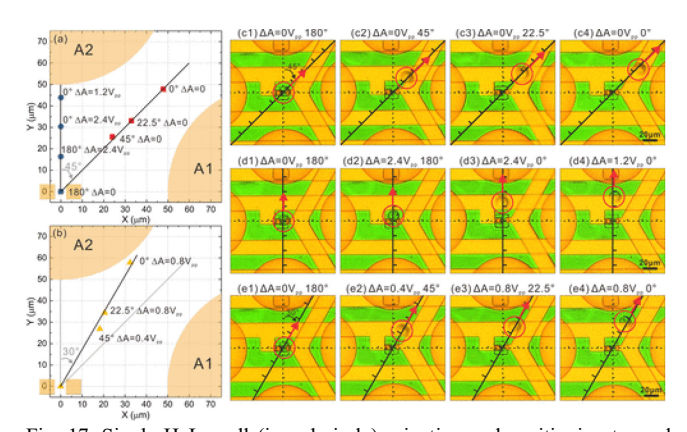


Fig. 17. Single HeLa cell (in red circle) orienting and positioning toward three directions $(0^\circ, 45^\circ, \text{ and } 30^\circ \text{ with the vertical line})$. (a) and (b) simulation result for the target positions. (c), (d), and (e) are the images of experimental results for the cell moving toward the three orientations, which are consistent with the simulation results (reprinted with permission from [84]).

V. FABRICATION PROCESS

As we mentioned before, the dielectrophoretic process can be achieved by the implementation of an electric field gradient through appropriate electrodes or a proper arrangement of insulators inside an electric field. This requires an accurate fabrication process for constructing specific pattern which is suitable for the purpose of manipulation such as trapping, separating, and transportation [79]. To enhance the DEP force, it is recommended to have sharp edges and small electrode separations rather than applying a high amplitude signal. This suggests a repeatable and precise fabrication process. For instance, when we are dealing with the trapping process, one possible method is the fabrication of at least a pair of conductive electrodes fitted to the dimension of the targeted material to assure a controlled trap instead of the aggregation of materials in the trap location. The use of microfabrication techniques facilitates the accurate fabrication of small features and accordingly guarantees the performance of the system with the lower operating voltages in the range of tens of volts for iDEP and a few volts for eDEP configurations [184]. In this section, we will discuss the fabrication methods and the focus is on the electrode fabrication for eDEP configuration and insulator arrangement and fabrication for iDEP

configuration.

A. Electrode fabrication

Electrode-based DEP devices require at least a pair of metallic electrodes to operate. Different metals such as gold, platinum, titanium, chromium, and aluminum or transparent conductors such as ITO are generally used in DEP process. Since gold and platinum have more biocompatibility and electrochemical stability, they are frequently used as electrode materials. Electron beam evaporator, thermal evaporator, and sputter machines are commonly used to deposit thin-film layers. Electrodes can be shaped either during or after the metal deposition. Usually, a shadow mask is used to form electrodes during the film deposition. A shadow mask is a metallic plate with patterns carved through the material. The shadow mask is positioned into close contact with the substrate in the deposition chamber. The target material is deposited through the patterns of a shadow mask onto the substrate. This is a simple and cheap process; however, it is not suitable for high-resolution applications, feature edges are not sharp, and the alignment process is difficult and not accurate. This process is not applicable for resolving features of less than tens of micrometers. To accurately pattern the deposited metal and resolve the electrode shapes "lift-off" or "etch-back" methods are utilized. The lift-off process is briefly shown in Fig. 18. The process starts with coating the substrate with a photoresist and the required pattern is transferred to the photoresist using the photolithography method or electronbeam lithography and developing process. Therefore, the surface of the substrate except the required pattern is covered with photoresist. After that, the thin film material is deposited onto the entire surface of the sample, covering both the photoresist and the generated pattern. Finally, the photoresist along with metal seated on top of it is lifted off of the substrate by releasing it using a specific chemical solvent for the photoresist, thus leaving the metallic pattern of electrodes on the substrate. For instance, a quadrupole electrode structure, which is shown in Fig. 13(a), was fabricated by patterning dual titanium-gold layers onto a glass slide. Photolithography is used to define the electrode patterns with photoresist Shipley AZ-5214. The process followed by evaporating 50 Å of titanium and 2500 Å of gold on the substrate. The process was completed after metal lift-off in acetone [166].

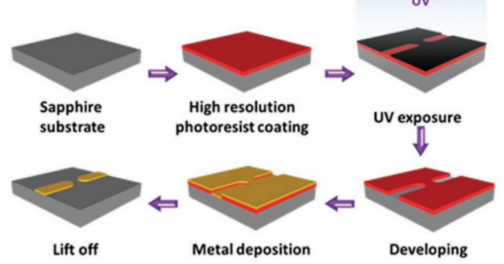


Fig. 18. Photolithography and lift-off process for fabricating nanoelectrodes (reprinted with permission from [65]).

The etch-back process is slightly different from lift-off. In this process, first, a metallic layer is deposited on the entire surface of the substrate, and then the unwanted parts are removed using special chemicals (wet etch process) or plasma (Dry etch process). Before performing the etching process, the required pattern is covered with a specific masking material to protect it from the etchant material. Depending on the process and type of the etchant, the masking material can be a photoresist that has been patterned using photolithography or a hard material such as silicon dioxide or silicon nitride. The etch-back technique can provide higher quality edges than the lift-off technique however the etchant materials used may react with or etch other materials or substrate of the sample.

In a study, a photolithography technique is used to fabricate a gap in the range of 10 µm and electrodes width of 1 mm on glass substrate [46]. In another study, a standard photolithography technique with a minimum feature size of 2 μm is used to fabricate DEP devices on a quartz substrate [15]. This device with a 12 µm gap and 2 µm electrode widths is used to trap wires 18 µm in length and 240 nm in diameter. The advantage of thin film metallic electrodes is that the fabrication process is highly developed in the integrated circuit industry and high yield devices for a variety of designs even for nanogaps and nanoelectrodes are achievable. The fabrication process for devices dealing with nanomaterials can be challenging since the electrode and gap size may need to be in the nanoscale range beyond the ability of high throughput fabrication processes such as the photolithography method. Some techniques are developed to deal with these structures. Electron-beam lithography is commonly used nanoelectrode or nanogap fabrication [69, 146]. In this process instead of light (which is used in photolithography), a focused electron beam is used to draw a pattern on a surface covered with an electron-sensitive film (resist). Electron beam lithography is a low-throughput and costly fabrication process and is only suitable for research activities as it lacks high throughput fabrication capabilities for real applications. However, as an alternative method, it is possible to fabricate bigger electrodes and incorporate a controlling mechanism to detect the presence of target materials in the gap and to prevent accumulation of nanomaterials in between the electrodes [65].

Three-dimensional electrodes are another arrangement that can be used to trap or filter materials such as biomolecules and cells. As mentioned before, this structure can increase the throughput of the system or deal with big materials. The electroplating technique is usually used to extrude metallic electrodes on the device. This process coats a metal on a substrate through the reduction of cations of that metal by means of a direct electric current produced by an external power supply. The substrate acts as the cathode; the electrolyte is a solution of a salt and the metal to be coated; and the anode is a conductive material. In this process, first, photolithography is required to define the area of electrodes. In a study, Voldman et al. fabricated 60-µm high electrodes to trap a single cell in between metallic pillars in a quadrupole structure [151].

As discussed, carbon electrodes and doped silicon electrodes are useful specifically to decrease the electrochemical or chemical reaction of the material with

Table 1. Advantages, limitations, and required manufacturing process of electrode materials.

Materials	Advantage	Limitation	Manufacturing process
Gold and platinum	Good electrochemical stability and biocompatibility	May electrochemically react with the sample if the voltage level is high	Photolithography and physical vapor deposition/sputtering techniques; Photolithography can be replaced by shadow mask (low resolution) or Electron-beam lithography (very high resolution, low-throughput, and expensive)
Indium tin oxide (ITO)	Transparent electrode	May electrochemically react with the sample if the voltage level is high	Photolithography and sputtering techniques. Photolithography can be replaced by shadow mask (low resolution)
Doped silicon	High electrochemical stability; High aspect ratio structures	High electrical resistivity; Complex and expensive fabrication process	Photolithography, diffusion / ion implantation, and deep reactive ion etching (DRIE) techniques
Carbon	High electrochemical stability; Outstanding biocompatibility; Simple and cheap fabrication process; High aspect ratio structures	High electrical resistivity; Limited choice of substrate; Expensive and nonflexible substrate; Small gap fabrication is not possible	Photolithography and pyrolysis steps
Metal coated diamond-like carbon electrodes	3D electrodes; Coating with highly doped silicon instead of metal coating increases electrochemical stability	Expensive fabrication process	Focused ion beam assisted chemical vapor deposition, plasma etching, and physical vapor deposition techniques
3D metallic electrodes	Increases the throughput of the system; Can deal with big materials	Expensive for precious metals	Photolithography and electroplating techniques
silver-NPs ink	Flexible, cheap, and fast method; Compatible with a wide variety of substrates	Low resolution	Printing technology

electrodes. Carbon electrodes have a simpler and cheaper fabrication process compared to metallic electrodes. Also, they offer the advantage of a wide range of electrochemical stability [59] and biocompatibility [60-63]. Accordingly, replacing the metallic electrodes in electrode-based DEP with carbon combines the advantages of both electrode-based DEP and iDEP. This means that the possibility of sample electrolysis decreases, and also lower voltages are required, compared to iDEP, to produce the required electric field gradient for the DEP process. The fabrication process is typically composed of photolithography and pyrolysis steps, as shown in Fig. 19. In this process first, an organic precursor such as SU-8 or AZ photoresist is patterned on the substrate by the photolithography technique. Then carbon electrodes form by pyrolyzing the patterned precursors at high temperatures up to 950°C in an inert atmosphere or vacuum [61]. This method provides a glassy carbon electrode with higher electrochemical stability and lower electrical conductivity than conductive carbon electrodes. Carbon electrodes with a height of a couple of hundreds of micrometers are reported with this technique [61, 63]. There are two challenges associated with the fabrication process of carbon electrodes. First, there is a limited choice for substrate since it should be able to tolerate the high temperature requires for the pyrolysis step. Flexible substrates are not the suitable choice but opaque silicon and fused silica are two examples of rigid substrates that are commonly used for this process [61]. The proper substrates for this technique are usually more expensive than normal substrates. Second, the predefined precursors shrink during the pyrolysis process, and therefore the dimension of the predefined pattern changes. The shrinkage rate depends on the type of the polymer and the original structure and fortunately, it is possible to calibrate the process [61, 185]. However, this problem can be a limiting factor for making a small gap between the electrodes. Since some 3D structures can be simply fabricated using this technique, it has specific application in DEP process. Dimondlike carbon is another stable material that is reported for 3D electrodes. However, the fabrication process is complex and expensive. The process started with defining the shape of the 3D nanoelectrode. For this purpose, they used focused ion beam assisted chemical vapour deposition to form diamondlike carbon (DLC) and then reshape it by post-plasma etching. The fabrication process continued by coating the DLC structure with a thin layer of aluminum to apply the DEP signal to the DLC structure [73]. Doped silicon is another material to decrease the electrochemical reaction effect [55, 56]. Although silicon process is well established, the fabrication process for this type of DEP device is complex and expensive since it required deep reactive ion etching to define the electrode structures on the highly doped silicon substrate [55].

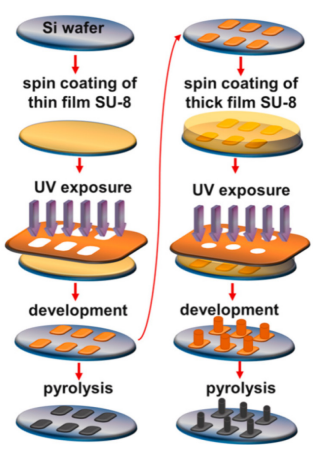


Fig. 19. a typical fabrication process for 2D and 3D carbon electrodes consisting of photolithography and pyrolysis steps (reprinted with permission from [58]).

Printing technology is another method that allows the high throughput fabrication of DEP devices. Although the achievable resolution of this technology is much lower than that of the discussed methods, printing technologies are more flexible, less expensive, and faster than the others discussed, and it is also compatible with a wide variety of substrates. As such, printing technology has received special attention in electronics, energy harvesting, sensors, and optoelectronics [186]. To the best of our knowledge, the best reported resolution is about 50 µm [187] and the resolution of hundreds of micrometers is easily achievable. An inkjet printing DEP device is reported for plankton separation. The interdigitated electrodes were printed on clean and dehydrated Polyethylene naphthalate (PEN) foils. Commercial silver-nanoparticles ink (PV-Nanocell I40DM-106) with 40% metal by weight was used as ink material. After printing, ink was cured and sintered in a convection oven at 180 °C for 1 h in an air atmosphere. The minimal electrode width was in the range from 90 to 150 µm with approximately 300 nm in height. Electrode spacing was set to 180 µm [81].

A variety of materials can be used for electrode fabrication based on the application, cost, and availability of the equipment. Table 1 summarized the advantages, limitations, and required manufacturing process of numerous electrode materials.

B. Insulator fabrication

As mentioned before, another substitute for electrode-based DEP is insulator-based DEP. iDEP can be either composed of an array of insulators or another specific arrangement of insulators to disturb the electric field for generating high non-uniformity in the electric field. In general, there is no need for fabricating specific micro and nanoelectrodes. As such, the fabrication process in most cases is simple and cheap. The common fabrication approach is to fill an array of insulators inside a fluidic channel. The insulators can be in the shape of rods, spheres, textiles, etc. in this case, a pair of electrodes can generate electric field across the channel and the presence of space and voids between the insulators provides

nonuniformity in the applied electric field. The electric field gradient is maximum in the contact point of the insulators [48, 91]. If there are enough minima and maxima in the electric field distribution, this device can be utilized as a filter to split different particles in a solution by trapping specific materials [156]. Since the insulators are readily available at inexpensive prices, the overall fabrication process is cheap and simple. Another methodology is to fabricate a specific predesigned insulator structures on a substrate. The fabrication process for these structures involves etching (wet or dry) for hard materials such as glass and silicon [125, 140] or injection molding or embossing for polymer-based materials [117]. The etching process of the hard materials requires a photolithography process to define the etch area and accordingly the unwanted parts of the substrate should be covered with a photoresistor metallic layer. Then wet/dry etching process can be applied to define the structure. It can be inferred that this method has an expensive fabrication process and there is no superiority to electrode-based DEP in terms of the fabrication process. However, if the fluidic channel is required to be implemented, both channel and insulator patterns can be fabricated in the same process with an excellent alignment. Injection molding and embossing techniques are the other approach with simple and costeffective fabrication process suitable for polymer-based materials. Polymer-based materials are more durable since they are not fragile. Polymers are produced with wide range of physical and chemical properties. This makes them a suitable candidate for variety of applications. The disadvantage of the polymer-based structures is that high aspect ratio structures are difficult to mold or stamp and microstructures in the range of 50 µm or below is not feasible to fabricate [188, 189]. Although the polymer-based fabrication process is simple and cheap, the drawback of the method is that the master mold requires a complicated and expensive process. This price can be acceptable if the master mold is used in the mass production process. Shafiee et al. reported an interesting iDEP structure made of PDMS polymer [190]. The structure consists of three fluidic channels. Electrodes are conductive liquids in two channels (electrode channels) that are not in direct contact with the main channels contains sample fluid. Electrodes are capacitively coupled to the main channel. In this structure, the required nonuniformity is generated by the geometry of the electrode channels. The fabrication process starts with pouring PDMS onto the silicon master and then curing for 45 min at 100°C. After removing the mold, fluidic connections to the channels were punched. Finally, the PDMS replica was bonded with the clean glass slides after treating with oxygen plasma.

Although electrodes do not play an important role in iDEP structure in generating the desired gradient for the electric field, they should be aligned well with the sample during the fabrication process. Usually, electrodes are fabricated in a separate step of the fabrication process and alignment is challenging unless an expensive fabrication process is utilized. The electrode misalignment causes a change in the experimental condition and significantly affects the

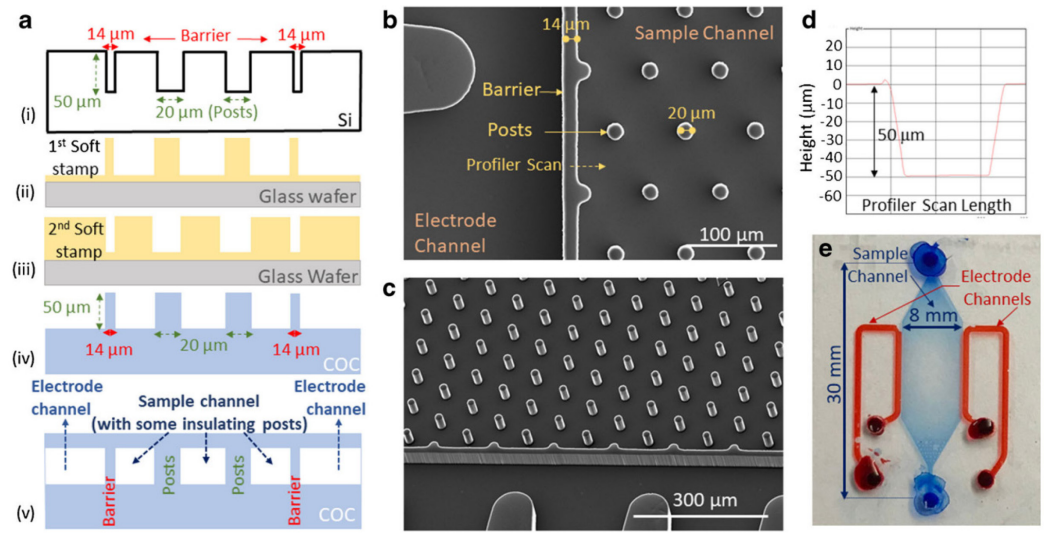


Fig. 20. (a) steps of the fabrication process. (b) Top and (c) tilted of the imprinted COC replica (SEM images) to show the membrane and post morphology. (d) Depths of 50 µm measured for the device cross-section using a stylus profilometry. (e) optical image of the fabricated device with liquid electrodes (red channels) and sample (blue chamber). (reprinted with permission from [1]).

reproducibility of the experiment. For instance, the thickness of the insulator layer between electrodes and the microfluidic chamber affects the coupling efficiency. As such, variation in thickness of this layer varies the coupling efficiency, and accordingly, the amplitude or frequency of the applied signal should be adjusted. This problem can be avoided if electrodes, insulators, and chambers are fabricated in a single layer without an alignment procedure. Salahi et al. presented an iDEP device that both the electrodes and the sample channel were fabricated simultaneously using a single-layer imprint and bonding process using a cyclic olefin copolymer [1]. In this design, the electrodes are separate microfluidic channels containing a conductive liquid with the interceding barrier layer (14-µm width and 50-µm depth). Since the device does not require solid electrodes the fabrication process is simple and efficient. Fig. 20(a) shows the fabrication process. The standard deep reactive ion etching (DRIE) method is used to create the high aspect ratio structures (50-µm depth and indicated lateral features) on a silicon wafer. This structure is used as a master mold. The positive image of the master mold was transferred to a soft stamp in two stamping processes (second soft stamp in Fig. 20(a)) using an appropriate UV curable polymer on glass wafers. This second soft stamp was then used to make the cyclic olefin copolymer (COC) replica by using the hot emboss imprinting and release technique. The imprinted COC channels were then encapsulated by bonding to a COC coverslip in a hot embosser.

VI. OUTLOOK

The research perspective in this field is to design practical, high throughput, and inexpensive devices that can reliably manipulate micro and nanomaterials. In particular, the desired DEP devices should (1) operate with low voltages to prevent any unwanted effects of the electric field or potential, charge transport to the sample, and Joule heating; (2) have a large electrochemical window to decrease electrochemical reactions between the electrodes and the samples in eDEP case; (3) have

inexpensive and straightforward fabrication processes for manufacturing; and (4) be able to manipulate sufficiently high sample volumes for practical applications.

Significant advances in DEP manipulation have been reported to achieve the mentioned goals. Now, DEP devices are more functional and have a variety of applications in wide ranging disciplines including medical diagnostics, micro and nanomaterial characterization, cell therapeutics, and particle filtration, and device fabrication. However, some areas require more attention to improve the usability, functionality, and availability of DEP devices. First, even though the operating voltage of the iDEP devices has significantly declined, the voltage is still unsuitably high for devices manufactured with simple fabrication processes. The operating voltage of most iDEP devices is hundreds of volts, which limits the device utility, and restricts portability as mobile power sources (such as a battery) will be short-lived. Second, the fabrication process for DEP devices designed for trapping 1D or 0D nanomaterials is typically slow and expensive. Although we introduce less expensive and high throughput fabrication processes for nanoparticle trapping systems supported by a monitoring circuit, more research is still required to extend this method for iDEP devices, to increase the variety of materials, and to develop it for wide implementation. Third, printing technologies are promising for flexible, inexpensive, and high throughput fabrication processes. To date, this technology has been shown to be suitable for fabricating DEP devices with the features down to tens of micrometers. Extensive research is required to improve the printing resolution to became suitable for dealing with nanoscale objects. Forth, material transportation can be useful for a variety of applications such as programmable micro and nanofabrication. Although substantial research has been reported for DEP process improvement, inexpensive transportation systems using the DEP force are still in their infancy. Finally, high throughput devices are in demand. For applications such as separation, filtering, and transportation,

increases in the manipulation speed are still needed. Although the increment of the device size or multiple device incorporation are methods for achieving this goal, a sophisticated solution such as using a crossover frequency for separating samples can improve the user-friendliness of the device.

Progress in DEP technology accelerates the improvement in fields such as medical diagnostics, material characterization, drug discovery, cell therapeutics, and particle filtration. A variety of technologies such as micro and nanofabrication, microfluidics, and inkjet printing are utilized to implement designed structures. Although many suitable devices are developed, still this field requires special attention to develop inexpensive and high throughput devices suitable for medical and industrial applications. Moreover, DEP technology can get the benefit of the emerging 3D printing technology. 3D printing technology has shown a promising platform for inexpensive, simple, and flexible fabrication processes. Recent advances in 3D printing technology in terms of printable materials and printing accuracy opens up various applications for this technology. Accordingly, in the future, fully integrated DEP structures or required master molds can be printed without the need for a cleanroom facility and complex fabrication processes. 3D-printed technology accelerates research in the DEP field by decreasing the fabrication time and expenses.

Moreover, DEP technology can potentially provide a suitable platform to facilitate the design of cheap, fast response, reliable, and high-efficiency laboratory equipment operating with a small volume of samples for performing various tests simultaneously. Specifically, DEP can enable efficient transportation, concentration, and separation of targeted materials toward the locations of interest in microfluidic chips. This approach can miniaturize bulky benchtop instruments. Although these systems require the involvement of different modules for signal generation, signal conditioning, data acquisition, data processing, and humanmachine interfaces, the current progress in semiconductor technology-enabled small scale, low consumption, and ultrafast electronics and processors. Even, daily used electronics such as cell phones and laptops carry powerful processors, reliable communication ports for signal generation and data acquisition, user-friendly human-machine interfaces, and dependable power sources that can be utilized for simplifying the design in order to develop portable labs on a chip.

VII. CONCLUSION

This study aimed to provide an overview of the DEP fundamentals, methodologies, device fabrication process, and material manipulation. Dielectrophoretic manipulation is based on a force that is applied to a polarizable material in the presence of a non-uniform electric field. Here, we discussed the two important methodologies including electrode-based DEP (eDEP) and insulator-based DEP (iDEP) to produce nonuniformity in electric field distribution. Depending on the process and the materials static field or dynamic field with a

specific frequency will be employed to have a reliable operation. The generated force can be used to trap, separate, and transport polarizable materials. we also reviewed the fabrication methods for eDEP and iDEP configurations.

REFERENCES

- [1] A. Salahi *et al.*, "Self-aligned microfluidic contactless dielectrophoresis device fabricated by single-layer imprinting on cyclic olefin copolymer," *Analytical and bioanalytical chemistry*, vol. 412, no. 16, pp. 3881-3889, 2020.
- [2] H. A. Pohl, "The motion and precipitation of suspensoids in divergent electric fields," *Journal of applied Physics*, vol. 22, no. 7, pp. 869-871, 1951.
- [3] R. Martinez-Duarte, "Microfabrication technologies in dielectrophoresis applications—A review," *Electrophoresis*, vol. 33, no. 21, pp. 3110-3132, 2012.
- [4] A. Nakano and A. Ros, "Protein dielectrophoresis: advances, challenges, and applications," *Electrophoresis*, vol. 34, no. 7, pp. 1085-1096, 2013.
- [5] W. H. De Jong and P. J. Borm, "Drug delivery and nanoparticles: applications and hazards," *International journal of nanomedicine*, vol. 3, no. 2, p. 133, 2008.
- [6] J. Castillo, S. Tanzi, M. Dimaki, and W. Svendsen, "Manipulation of self-assembly amyloid peptide nanotubes by dielectrophoresis," *Electrophoresis*, vol. 29, no. 24, pp. 5026-5032, 2008.
- [7] T. Ghomian, O. Kizilkaya, and J.-W. Choi, "Lead sulfide colloidal quantum dot photovoltaic cell for energy harvesting from human body thermal radiation," *Applied energy*, vol. 230, pp. 761-768, 2018.
- [8] G. Zhu et al., "Toward large-scale energy harvesting by a nanoparticle-enhanced triboelectric nanogenerator," Nano letters, vol. 13, no. 2, pp. 847-853, 2013.
- [9] C. E. McCold, Q. Fu, J. Y. Howe, and J. Hihath, "Conductance based characterization of structure and hopping site density in 2D molecule-nanoparticle arrays," *Nanoscale*, vol. 7, no. 36, pp. 14937-14945, 2015.
- [10] T. Ghomian and S. Mehraeen, "Survey of energy scavenging for wearable and implantable devices," *Energy*, vol. 178, pp. 33-49, 2019
- [11] S. Baruah and J. Dutta, "Nanotechnology applications in pollution sensing and degradation in agriculture: a review," *Environmental Chemistry Letters*, vol. 7, no. 3, pp. 191-204, 2009.
- [12] A. D. Servin and J. C. White, "Nanotechnology in agriculture: next steps for understanding engineered nanoparticle exposure and risk," *NanoImpact*, vol. 1, pp. 9-12, 2016.
- [13] T. Ghomian, S. Farimand, and J.-W. Choi, "The effect of isopropylamine-capped PbS quantum dots on infrared photodetectors and photovoltaics," *Microelectronic Engineering*, vol. 183, pp. 48-51, 2017.
- [14] H. Monsef and T. Ghomian, "Modified quadrature method for accurate voltage measurement in optical voltage transducer," *IEE Proceedings-Generation, Transmission and Distribution*, vol. 153, no. 5, pp. 524-530, 2006.
- [15] E. M. Freer, O. Grachev, X. Duan, S. Martin, and D. P. Stumbo, "High-yield self-limiting single-nanowire assembly with dielectrophoresis," *Nature nanotechnology*, vol. 5, no. 7, pp. 525-530, 2010.
- [16] T. Ghomian and S. Mehraeen, "A hybrid structure for energy harvesting from human body thermal radiation and mechanical movement," *Przegląd Elektrotechniczny*, vol. 95, 2019.
- [17] G. D'Ambrogio et al., "Structuring BaTiO3/PDMS nanocomposite via dielectrophoresis for fractional flow reserve measurement," Advanced Engineering Materials, 2021.
- [18] T. Ghomian, N. Darwish, and J. Hihath, "Thickness-Dependent Seebeck Coefficient in Hybrid 2-Dimensional layers," in 2021 IEEE 16th Nanotechnology Materials and Devices Conference (NMDC), 2021: IEEE, pp. 1-4.
- [19] H. H. Kung and M. C. Kung, "Nanotechnology: applications and potentials for heterogeneous catalysis," *Catalysis today*, vol. 97, no. 4, pp. 219-224, 2004.

[48]

- [20] D. L. Giokas, A. G. Vlessidis, G. Z. Tsogas, and N. P. Evmiridis, "Nanoparticle-assisted chemiluminescence and its applications in analytical chemistry," *TrAC Trends in Analytical Chemistry*, vol. 29, no. 10, pp. 1113-1126, 2010.
- [21] J. Marrs, T. Ghomian, L. Domulevicz, C. McCold, and J. Hihath, "Gold Nanoparticle Synthesis," *JoVE (Journal of Visualized Experiments)*, no. 173, p. e62176, 2021.
- [22] P. H. Jones, O. M. Marago, and G. Volpe, *Optical tweezers: Principles and applications*. Cambridge University Press, 2015.
- [23] R. Pethig, "Dielectrophoresis: Status of the theory, technology, and applications," *Biomicrofluidics*, vol. 4, no. 2, p. 022811, 2010.
- [24] S. N. Varanakkottu, S. D. George, T. Baier, S. Hardt, M. Ewald, and M. Biesalski, "Particle manipulation based on optically controlled free surface hydrodynamics," *Angewandte Chemie International Edition*, vol. 52, no. 28, pp. 7291-7295, 2013.
- [25] M. A. Andrade, N. Pérez, and J. C. Adamowski, "Particle manipulation by a non-resonant acoustic levitator," *Applied physics letters*, vol. 106, no. 1, p. 014101, 2015.
- [26] B. Shao, S. Zlatanovic, M. Ozkan, A. L. Birkbeck, and S. C. Esener, "Manipulation of microspheres and biological cells with multiple agile VCSEL traps," *Sensors and Actuators B: Chemical*, vol. 113, no. 2, pp. 866-874, 2006.
- [27] S. Yu et al., "On-chip optical tweezers based on freeform optics," Optica, vol. 8, no. 3, pp. 409-414, 2021.
- [28] C. Renaut *et al.*, "On chip shapeable optical tweezers," *Scientific reports*, vol. 3, no. 1, pp. 1-4, 2013.
- [29] C. Chen *et al.*, "Enhanced optical trapping and arrangement of nano-objects in a plasmonic nanocavity," *Nano letters*, vol. 12, no. 1, pp. 125-132, 2012.
- [30] M. Tanyeri and C. M. Schroeder, "Manipulation and confinement of single particles using fluid flow," *Nano letters*, vol. 13, no. 6, pp. 2357-2364, 2013.
- [31] P. Y. Chiou, A. T. Ohta, and M. C. Wu, "Massively parallel manipulation of single cells and microparticles using optical images," *Nature*, vol. 436, no. 7049, pp. 370-372, 2005.
- [32] U. G. Būtaitė, G. M. Gibson, Y.-L. D. Ho, M. Taverne, J. M. Taylor, and D. B. Phillips, "Indirect optical trapping using light driven micro-rotors for reconfigurable hydrodynamic manipulation," *Nature communications*, vol. 10, no. 1, pp. 1-10, 2019.
- [33] T. Lilliehorn *et al.*, "Trapping of microparticles in the near field of an ultrasonic transducer," *Ultrasonics*, vol. 43, no. 5, pp. 293-303, 2005
- [34] B. Shen, V. Linko, H. Dietz, and J. J. Toppari, "Dielectrophoretic trapping of multilayer DNA origami nanostructures and DNA origami-induced local destruction of silicon dioxide," *Electrophoresis*, vol. 36, no. 2, pp. 255-262, 2015.
- [35] L. Ying, S. S. White, A. Bruckbauer, L. Meadows, Y. E. Korchev, and D. Klenerman, "Frequency and voltage dependence of the dielectrophoretic trapping of short lengths of DNA and dCTP in a nanopipette," *Biophysical journal*, vol. 86, no. 2, pp. 1018-1027, 2004.
- [36] R. Hölzel, N. Calander, Z. Chiragwandi, M. Willander, and F. F. Bier, "Trapping single molecules by dielectrophoresis," *Physical review letters*, vol. 95, no. 12, p. 128102, 2005.
- [37] C. L. Asbury, A. H. Diercks, and G. van den Engh, "Trapping of DNA by dielectrophoresis," *Electrophoresis*, vol. 23, no. 16, pp. 2658-2666, 2002.
- [38] S. Tuukkanen et al., "Trapping of 27 bp-8 kbp DNA and immobilization of thiol-modified DNA using dielectrophoresis," Nanotechnology, vol. 18, no. 29, p. 295204, 2007.
- [39] M. Kumemura et al., "Single-DNA-molecule trapping with silicon nanotweezers using pulsed dielectrophoresis," Journal of Micromechanics and microengineering, vol. 21, no. 5, p. 054020, 2011
- [40] B. H. Lapizco-Encinas and M. Rito-Palomares, "Dielectrophoresis for the manipulation of nanobioparticles," *Electrophoresis*, vol. 28, no. 24, pp. 4521-4538, 2007.
- [41] H. Morgan, M. P. Hughes, and N. G. Green, "Separation of submicron bioparticles by dielectrophoresis," *Biophysical journal*, vol. 77, no. 1, pp. 516-525, 1999.
- [42] R. R. Pethig, Dielectrophoresis: Theory, methodology and biological applications. John Wiley & Sons, 2017.
- [43] E. A. Kwizera, M. Sun, A. M. White, J. Li, and X. He, "Methods of Generating Dielectrophoretic Force for Microfluidic

- Manipulation of Bioparticles," ACS Biomaterials Science & Engineering, vol. 7, no. 6, pp. 2043-2063, 2021.
- [44] M. Viefhues and R. Eichhorn, "DNA dielectrophoresis: Theory and applications a review," *Electrophoresis*, vol. 38, no. 11, pp. 1483-1506, 2017.
- [45] W. Cao and K. A. Brown, "Theory for hierarchical assembly with dielectrophoresis and the role of particle anisotropy," *Electrophoresis*, vol. 42, no. 5, pp. 635-643, 2021.
- [46] C. M. White, L. A. Holland, and P. Famouri, "Application of capillary electrophoresis to predict crossover frequency of polystyrene particles in dielectrophoresis," *Electrophoresis*, vol. 31, no. 15, pp. 2664-2671, 2010.
- [47] M. P. Hughes, "Nanoelectromechanics," 2003.
 - L. Benguigui and I. Lin, "Phenomenological aspect of particle trapping by dielectrophoresis," *Journal of applied physics*, vol. 56, no. 11, pp. 3294-3297, 1984.
- [49] T. B. Jones, "Dielectrophoretic force calculation," *Journal of Electrostatics*, vol. 6, no. 1, pp. 69-82, 1979.
- [50] A. Jaffe and J. Voldman, "Multi-frequency dielectrophoretic characterization of single cells," *Microsystems & nanoengineering*, vol. 4, no. 1, pp. 1-9, 2018.
- [51] S. Tada, Y. Omi, and M. Eguchi, "Analysis of the dielectrophoretic properties of cells using the isomotive AC electric field," *Biomicrofluidics*, vol. 12, no. 4, p. 044103, 2018.
- [52] S. Mahabadi, F. H. Labeed, and M. P. Hughes, "Dielectrophoretic analysis of treated cancer cells for rapid assessment of treatment efficacy," *Electrophoresis*, vol. 39, no. 8, pp. 1104-1110, 2018.
- [53] D. P. Heineck, B. Sarno, S. Kim, and M. Heller, "Electrochemical attack and corrosion of platinum electrodes in dielectrophoretic diagnostic devices," *Analytical and bioanalytical chemistry*, vol. 412, no. 16, pp. 3871-3880, 2020.
- [54] A. Gencoglu and A. Minerick, "Chemical and morphological changes on platinum microelectrode surfaces in AC and DC fields with biological buffer solutions," *Lab on a Chip*, vol. 9, no. 13, pp. 1866-1873, 2009.
- [55] C. Iliescu, G. L. Xu, V. Samper, and F. E. Tay, "Fabrication of a dielectrophoretic chip with 3D silicon electrodes," *Journal of Micromechanics and Microengineering*, vol. 15, no. 3, p. 494, 2004
- [56] C. Iliescu, G. L. Xu, P. L. Ong, and K. J. Leck, "Dielectrophoretic separation of biological samples in a 3D filtering chip," *Journal of Micromechanics and Microengineering*, vol. 17, no. 7, p. S128, 2007.
- [57] X. Zhu, K.-W. Tung, and P.-Y. Chiou, "Heavily doped silicon electrode for dielectrophoresis in high conductivity media," *Applied Physics Letters*, vol. 111, no. 14, p. 143506, 2017.
- [58] S. Forouzanfar, N. Pala, M. Madou, and C. Wang, "Perspectives on C-MEMS and C-NEMS biotech applications," *Biosensors and Bioelectronics*, p. 113119, 2021.
- [59] W. Van der Linden and J. W. Dieker, "Glassy carbon as electrode material in electro-analytical chemistry," *Analytica Chimica Acta*, vol. 119, no. 1, pp. 1-24, 1980.
- [60] G. T. Teixidor et al., "Carbon microelectromechanical systems as a substratum for cell growth," *Biomedical Materials*, vol. 3, no. 3, p. 034116, 2008.
- [61] R. Martinez-Duarte, P. Renaud, and M. J. Madou, "A novel approach to dielectrophoresis using carbon electrodes," *Electrophoresis*, vol. 32, no. 17, pp. 2385-2392, 2011.
- [62] M. d. C. Jaramillo, E. Torrents, R. Martínez-Duarte, M. J. Madou, and A. Juárez, "On-line separation of bacterial cells by carbon-electrode dielectrophoresis," *Electrophoresis*, vol. 31, no. 17, pp. 2921-2928, 2010.
- [63] R. Martinez-Duarte, R. A. Gorkin III, K. Abi-Samra, and M. J. Madou, "The integration of 3D carbon-electrode dielectrophoresis on a CD-like centrifugal microfluidic platform," *Lab on a Chip*, vol. 10, no. 8, pp. 1030-1043, 2010.
- [64] R. C. Gallo-Villanueva, C. E. Rodríguez-López, R. I. Díaz-de-la-Garza, C. Reyes-Betanzo, and B. H. Lapizco-Encinas, "DNA manipulation by means of insulator-based dielectrophoresis employing direct current electric fields," *Electrophoresis*, vol. 30, no. 24, pp. 4195-4205, 2009.
- [65] T. Ghomian et al., "High-Throughput Dielectrophoretic Trapping and Detection of DNA Origami," Advanced Materials Interfaces, vol. 8, no. 5, p. 2001476, 2021.

- [66] R. Pethig, Y. Huang, X.-B. Wang, and J. P. Burt, "Positive and negative dielectrophoretic collection of colloidal particles using interdigitated castellated microelectrodes," *Journal of Physics D: Applied Physics*, vol. 25, no. 5, p. 881, 1992.
- [67] J. Yang, Y. Huang, X.-B. Wang, F. F. Becker, and P. R. Gascoyne, "Cell separation on microfabricated electrodes using dielectrophoretic/gravitational field-flow fractionation," *Analytical chemistry*, vol. 71, no. 5, pp. 911-918, 1999.
- [68] M. Olariu, A. Arcire, and M. E. Plonska-Brzezinska, "Controlled trapping of onion-like carbon (OLC) via dielectrophoresis," *Journal of Electronic Materials*, vol. 46, no. 1, pp. 443-450, 2017.
- [69] N. G. Green, H. Morgan, and J. J. Milner, "Manipulation and trapping of sub-micron bioparticles using dielectrophoresis," *Journal of Biochemical and Biophysical Methods*, vol. 35, no. 2, pp. 89-102, 1997.
- [70] Y. Huang, R. Holzel, R. Pethig, and X.-B. Wang, "Differences in the AC electrodynamics of viable and non-viable yeast cells determined through combined dielectrophoresis and electrorotation studies," *Physics in Medicine & Biology*, vol. 37, no. 7, p. 1499, 1992.
- [71] P. Pham *et al.*, "Numerical design of a 3-D microsystem for bioparticle dielectrophoresis: The Pyramidal Microdevice," *Journal of Electrostatics*, vol. 65, no. 8, pp. 511-520, 2007.
- [72] Y. Huang and R. Pethig, "Electrode design for negative dielectrophoresis," *Measurement Science and Technology*, vol. 2, no. 12, p. 1142, 1991.
- [73] T. Yamamoto and T. Fujii, "Active immobilization of biomolecules on a hybrid three-dimensional nanoelectrode by dielectrophoresis for single-biomolecule study," *Nanotechnology*, vol. 18, no. 49, p. 495503, 2007.
- [74] A. Kuzyk, "Dielectrophoresis at the nanoscale," *electrophoresis*, vol. 32, no. 17, pp. 2307-2313, 2011.
- [75] W. Liu, C. Wang, H. Ding, J. Shao, and Y. Ding, "AC electric field induced dielectrophoretic assembly behavior of gold nanoparticles in a wide frequency range," *Applied Surface Science*, vol. 370, pp. 184-192, 2016
- [76] D. Kim, M. Sonker, and A. Ros, "Dielectrophoresis: From molecular to micrometer-scale analytes," *Analytical chemistry*, vol. 91, no. 1, pp. 277-295, 2018.
- [77] J. R. Gong, "Label-free attomolar detection of proteins using integrated nanoelectronic and electrokinetic devices," *small*, vol. 6, no. 8, pp. 967-973, 2010.
- [78] C. Zhang, K. Khoshmanesh, A. Mitchell, and K. Kalantar-Zadeh, "Dielectrophoresis for manipulation of micro/nano particles in microfluidic systems," *Analytical and bioanalytical chemistry*, vol. 396, no. 1, pp. 401-420, 2010.
- [79] B. J. Kirby, Micro-and nanoscale fluid mechanics: transport in microfluidic devices. Cambridge university press, 2010.
- [80] H. J. Kim, J. Kim, Y. K. Yoo, J. H. Lee, J. H. Park, and K. S. Hwang, "Sensitivity improvement of an electrical sensor achieved by control of biomolecules based on the negative dielectrophoretic force," *Biosensors and Bioelectronics*, vol. 85, pp. 977-985, 2016.
- [81] L. Challier et al., "Printed Dielectrophoretic Electrode-Based Continuous Flow Microfluidic Systems for Particles 3D-Trapping," Particle & Particle Systems Characterization, vol. 38, no. 2, p. 2000235, 2021.
- [82] N. G. Green, A. Ramos, and H. Morgan, "Ac electrokinetics: a survey of sub-micrometre particle dynamics," *Journal of Physics D: Applied Physics*, vol. 33, no. 6, p. 632, 2000.
- [83] D. J. Bakewell, M. P. Hughes, J. J. Milner, and H. Morgan, "Dielectrophoretic manipulation of avidin and DNA," in Proceedings of the 20th Annual International Conference of the IEEE Engineering in Medicine and Biology Society. Vol. 20 Biomedical Engineering Towards the Year 2000 and Beyond (Cat. No. 98CH36286), 1998, vol. 2: IEEE, pp. 1079-1082.
- [84] T. Zheng, Z. Zhang, and R. Zhu, "Flexible trapping and manipulation of single cells on a chip by modulating phases and amplitudes of electrical signals applied onto microelectrodes," *Analytical chemistry*, vol. 91, no. 7, pp. 4479-4487, 2019.
- [85] A. Dalili et al., "Parametric study on the geometrical parameters of a lab-on-a-chip platform with tilted planar electrodes for continuous dielectrophoretic manipulation of microparticles," *Scientific reports*, vol. 10, no. 1, pp. 1-11, 2020.

- [86] S. Fiedler, S. G. Shirley, T. Schnelle, and G. Fuhr, "Dielectrophoretic sorting of particles and cells in a microsystem," *Analytical chemistry*, vol. 70, no. 9, pp. 1909-1915, 1998.
- [87] M. Islam, D. Keck, J. Gilmore, and R. Martinez-Duarte, "Characterization of the dielectrophoretic response of different candida strains using 3d carbon microelectrodes," *Micromachines*, vol. 11, no. 3, p. 255, 2020.
- [88] P. Puri, V. Kumar, S. Belgamwar, and N. Sharma, "Microfluidic device for cell trapping with carbon electrodes using dielectrophoresis," *Biomedical microdevices*, vol. 20, no. 4, pp. 1-10, 2018.
- [89] M. Elitas, Y. Yildizhan, M. Islam, R. Martinez-Duarte, and D. Ozkazanc, "Dielectrophoretic characterization and separation of monocytes and macrophages using 3D carbon-electrodes," *Electrophoresis*, vol. 40, no. 2, pp. 315-321, 2019.
- [90] S. K. Srivastava, A. Gencoglu, and A. R. Minerick, "DC insulator dielectrophoretic applications in microdevice technology: a review," *Analytical and bioanalytical chemistry*, vol. 399, no. 1, pp. 301-321, 2011.
- [91] I. Lin and L. Benguigui, "High-intensity, high-gradient electric separation and dielectric filtration of particulate and granular materials," *Journal of Electrostatics*, vol. 13, no. 3, pp. 257-278, 1982
- [92] B. A. Simmons, G. J. McGraw, R. V. Davalos, G. J. Fiechtner, Y. Fintschenko, and E. B. Cummings, "The development of polymeric devices as dielectrophoretic separators and concentrators," MRS bulletin, vol. 31, no. 2, pp. 120-124, 2006.
- [93] J. Regtmeier, R. Eichhorn, M. Viefhues, L. Bogunovic, and D. Anselmetti, "Electrodeless dielectrophoresis for bioanalysis: Theory, devices and applications," *Electrophoresis*, vol. 32, no. 17, pp. 2253-2273, 2011.
- [94] J. Zhu, T. R. J. Tzeng, and X. Xuan, "Continuous dielectrophoretic separation of particles in a spiral microchannel," *Electrophoresis*, vol. 31, no. 8, pp. 1382-1388, 2010.
- [95] Y. Kang, D. Li, S. A. Kalams, and J. E. Eid, "DC-Dielectrophoretic separation of biological cells by size," *Biomedical microdevices*, vol. 10, no. 2, pp. 243-249, 2008.
- [96] J. Zhu and X. Xuan, "Particle electrophoresis and dielectrophoresis in curved microchannels," *Journal of colloid and interface science*, vol. 340, no. 2, pp. 285-290, 2009.
- [97] S. K. Srivastava, P. R. Daggolu, S. C. Burgess, and A. R. Minerick, "Dielectrophoretic characterization of erythrocytes: Positive ABO blood types," *Electrophoresis*, vol. 29, no. 24, pp. 5033-5046, 2008.
- [98] K. H. Kang, Y. Kang, X. Xuan, and D. Li, "Continuous separation of microparticles by size with Direct current-dielectrophoresis," *Electrophoresis*, vol. 27, no. 3, pp. 694-702, 2006.
- [99] S. Masuda, M. Washizu, and T. Nanba, "Novel method of cell fusion in field constriction area in fluid integration circuit," *IEEE transactions on industry applications*, vol. 25, no. 4, pp. 732-737, 1989.
- [100] M. Gel, Y. Kimura, O. Kurosawa, H. Oana, H. Kotera, and M. Washizu, "Dielectrophoretic cell trapping and parallel one-to-one fusion based on field constriction created by a micro-orifice array," *Biomicrofluidics*, vol. 4, no. 2, p. 022808, 2010.
- [101] E. B. Cummings and A. K. Singh, "Dielectrophoretic trapping without embedded electrodes," in *Microfluidic Devices and Systems III*, 2000, vol. 4177: International Society for Optics and Photonics, pp. 151-160.
- [102] C.-F. Chou *et al.*, "Electrodeless dielectrophoresis of single-and double-stranded DNA," *Biophysical journal*, vol. 83, no. 4, pp. 2170-2179, 2002.
- [103] L. Gan, T.-C. Chao, F. Camacho-Alanis, and A. Ros, "Six-helix bundle and triangle DNA origami insulator-based dielectrophoresis," *Analytical chemistry*, vol. 85, no. 23, pp. 11427-11434, 2013.
- [104] A. Nakano, F. Camacho-Alanis, and A. Ros, "Insulator-based dielectrophoresis with β-galactosidase in nanostructured devices," *Analyst*, vol. 140, no. 3, pp. 860-868, 2015.
- [105] A. Nakano, F. Camacho-Alanis, T.-C. Chao, and A. Ros, "Tuning direct current streaming dielectrophoresis of proteins," *Biomicrofluidics*, vol. 6, no. 3, p. 034108, 2012.
- [106] B. G. Abdallah, S. Roy-Chowdhury, J. Coe, P. Fromme, and A. Ros, "High throughput protein nanocrystal fractionation in a

- microfluidic sorter," *Analytical chemistry*, vol. 87, no. 8, pp. 4159-4167, 2015.
- [107] B. G. Abdallah *et al.*, "Microfluidic sorting of protein nanocrystals by size for X-ray free-electron laser diffraction," *Structural Dynamics*, vol. 2, no. 4, p. 041719, 2015.
- [108] J. Luo, B. G. Abdallah, G. G. Wolken, E. A. Arriaga, and A. Ros, "Insulator-based dielectrophoresis of mitochondria," *Biomicrofluidics*, vol. 8, no. 2, p. 021801, 2014.
- [109] J. Luo, K. A. Muratore, E. A. Arriaga, and A. Ros, "Deterministic absolute negative mobility for micro-and submicrometer particles induced in a microfluidic device," *Analytical chemistry*, vol. 88, no. 11, pp. 5920-5927, 2016.
- [110] M. T. Rabbani, C. F. Schmidt, and A. Ros, "Single-walled carbon nanotubes probed with insulator-based dielectrophoresis," *Analytical chemistry*, vol. 89, no. 24, pp. 13235-13244, 2017.
- [111] J. Suehiro, G. Zhou, M. Imamura, and M. Hara, "Dielectrophoretic filter for separation and recovery of biological cells in water," *IEEE Transactions on Industry Applications*, vol. 39, no. 5, pp. 1514-1521, 2003.
- [112] C. J. Evenhuis and P. R. Haddad, "Joule heating effects and the experimental determination of temperature during CE," *Electrophoresis*, vol. 30, no. 5, pp. 897-909, 2009.
- [113] R. C. Gallo-Villanueva, M. B. Sano, B. H. Lapizco-Encinas, and R. V. Davalos, "Joule heating effects on particle immobilization in insulator-based dielectrophoretic devices," *Electrophoresis*, vol. 35, no. 2-3, pp. 352-361, 2014.
- [114] X. Xuan, "Joule heating in electrokinetic flow," *Electrophoresis*, vol. 29, no. 1, pp. 33-43, 2008.
- [115] X. Xuan, B. Xu, D. Sinton, and D. Li, "Electroosmotic flow with Joule heating effects," *Lab on a Chip*, vol. 4, no. 3, pp. 230-236, 2004.
- [116] V. Chaurey, A. Rohani, Y. H. Su, K. T. Liao, C. F. Chou, and N. S. Swami, "Scaling down constriction-based (electrodeless) dielectrophoresis devices for trapping nanoscale bioparticles in physiological media of high-conductivity," *Electrophoresis*, vol. 34, no. 7, pp. 1097-1104, 2013.
- [117] W. A. Braff, A. Pignier, and C. R. Buie, "High sensitivity three-dimensional insulator-based dielectrophoresis," *Lab on a Chip*, vol. 12, no. 7, pp. 1327-1331, 2012.
- [118] B. G. Hawkins and B. J. Kirby, "Electrothermal flow effects in insulating (electrodeless) dielectrophoresis systems," *Electrophoresis*, vol. 31, no. 22, pp. 3622-3633, 2010.
- [119] Y. Yan, D. Guo, and S. Wen, "Joule heating effects on two-phase flows in dielectrophoresis microchips," *BioChip Journal*, vol. 11, no. 3, pp. 196-205, 2017.
- [120] R. A. Prabhakaran *et al.*, "Joule heating effects on electroosmotic entry flow," *Electrophoresis*, vol. 38, no. 5, pp. 572-579, 2017.
- [121] A. Nakano, J. Luo, and A. Ros, "Temporal and spatial temperature measurement in insulator-based dielectrophoretic devices," *Analytical chemistry*, vol. 86, no. 13, pp. 6516-6524, 2014.
- [122] A. Kale, S. Patel, G. Hu, and X. Xuan, "Numerical modeling of J oule heating effects in insulator-based dielectrophoresis microdevices," *Electrophoresis*, vol. 34, no. 5, pp. 674-683, 2013.
- [123] J. Zhu, S. Sridharan, G. Hu, and X. Xuan, "Joule heating effects on electrokinetic focusing and trapping of particles in constriction microchannels," *Journal of Micromechanics and Microengineering*, vol. 22, no. 7, p. 075011, 2012.
- [124] P. Zellner and M. Agah, "Silicon insulator-based dielectrophoresis devices for minimized heating effects," *Electrophoresis*, vol. 33, no. 16, pp. 2498-2507, 2012.
- [125] D. Nakidde et al., "Three dimensional passivated-electrode insulator-based dielectrophoresis," Biomicrofluidics, vol. 9, no. 1, p. 014125, 2015.
- [126] S. Soltanian-Zadeh, K. Kikkeri, A. N. Shajahan-Haq, J. Strobl, R. Clarke, and M. Agah, "Breast cancer cell obatoclax response characterization using passivated-electrode insulator-based dielectrophoresis," *Electrophoresis*, vol. 38, no. 16, pp. 1988-1995, 2017.
- [127] V. H. Perez-Gonzalez, R. C. Gallo-Villanueva, B. Cardenas-Benitez, S. O. Martinez-Chapa, and B. H. Lapizco-Encinas, "Simple approach to reducing particle trapping voltage in insulator-based dielectrophoretic systems," *Analytical chemistry*, vol. 90, no. 7, pp. 4310-4315, 2018.
- [128] M. Sun, P. Agarwal, S. Zhao, Y. Zhao, X. Lu, and X. He, "Continuous on-chip cell separation based on conductivity-induced

- dielectrophoresis with 3D self-assembled ionic liquid electrodes," *Analytical chemistry*, vol. 88, no. 16, pp. 8264-8271, 2016.
- [129] M. L. Kovarik and S. C. Jacobson, "Integrated nanopore/microchannel devices for ac electrokinetic trapping of particles," *Analytical chemistry*, vol. 80, no. 3, pp. 657-664, 2008.
- [130] G. R. Pesch et al., "Recovery of submicron particles using high-throughput dielectrophoretically switchable filtration," Separation and Purification Technology, vol. 132, pp. 728-735, 2014.
- [131] F. Du *et al.*, "Fouling suppression in submerged membrane bioreactors by obstacle dielectrophoresis," *Journal of Membrane science*, vol. 549, pp. 466-473, 2018.
- [132] Y. K. Cho, S. Kim, K. Lee, C. Park, J. G. Lee, and C. Ko, "Bacteria concentration using a membrane type insulator-based dielectrophoresis in a plastic chip," *Electrophoresis*, vol. 30, no. 18, pp. 3153-3159, 2009.
- [133] B. H. Lapizco-Encinas, "On the recent developments of insulator-based dielectrophoresis: A review," *Electrophoresis*, vol. 40, no. 3, pp. 358-375, 2019.
- [134] H. Mukaibo et al., "Ultrathin nanoporous membranes for insulator-based dielectrophoresis," Nanotechnology, vol. 29, no. 23, p. 235704, 2018.
- [135] L. Liu, K. Chen, N. Xiang, and Z. Ni, "Dielectrophoretic manipulation of nanomaterials: A review," *Electrophoresis*, vol. 40, no. 6, pp. 873-889, 2019.
- [136] E. T. Vandenberg *et al.*, "Structure of 3-aminopropyl triethoxy silane on silicon oxide," *Journal of colloid and interface science*, vol. 147, no. 1, pp. 103-118, 1991.
- [137] T. Wada, K. Yamazaki, T. Isono, and T. Ogino, "Characterization of local hydrophobicity on sapphire (0001) surfaces in aqueous environment by colloidal probe atomic force microscopy," *Applied Surface Science*, vol. 396, pp. 1206-1211, 2017.
- [138] T. Isono, T. Ikeda, R. Aoki, K. Yamazaki, and T. Ogino, "Structural-and chemical-phase-separation on single crystalline sapphire (0001) surfaces," *Surface science*, vol. 604, no. 21-22, pp. 2055-2063, 2010.
- [139] E. O. Adekanmbi and S. K. Srivastava, "Dielectrophoretic applications for disease diagnostics using lab-on-a-chip platforms," *Lab on a Chip*, vol. 16, no. 12, pp. 2148-2167, 2016.
- [140] P. Zellner et al., "3D Insulator-based dielectrophoresis using DC-biased, AC electric fields for selective bacterial trapping," Electrophoresis, vol. 36, no. 2, pp. 277-283, 2015.
- [141] S. Patel, D. Showers, P. Vedantam, T.-R. Tzeng, S. Qian, and X. Xuan, "Microfluidic separation of live and dead yeast cells using reservoir-based dielectrophoresis," *Biomicrofluidics*, vol. 6, no. 3, p. 034102, 2012.
- [142] J. Zhu, G. Hu, and X. Xuan, "Electrokinetic particle entry into microchannels," *Electrophoresis*, vol. 33, no. 6, pp. 916-922, 2012.
- [143] A. Kale, S. Patel, and X. Xuan, "Three-dimensional reservoir-based dielectrophoresis (rDEP) for enhanced particle enrichment," *Micromachines*, vol. 9, no. 3, p. 123, 2018.
- [144] A. Barik et al., "Nanogap dielectrophoresis combined with buffer exchange for detecting protein binding to trapped bioparticles," Colloids and Surfaces A: Physicochemical and Engineering Aspects, vol. 611, p. 125829, 2021.
- [145] Y. A. Sadabad, A. Khodadadian, K. H. Istadeh, M. Hedayati, R. Kalantarinejad, and C. Heitzinger, "Frequency dependence of dielectrophoretic fabrication of single-walled carbon nanotube field-effect transistors," *Journal of Computational Electronics*, vol. 19, no. 4, pp. 1516-1526, 2020.
- [146] A. Kuzyk, B. Yurke, J. J. Toppari, V. Linko, and P. Törmä, "Dielectrophoretic trapping of DNA origami," *Small*, vol. 4, no. 4, pp. 447-450, 2008.
- [147] L. An and C. R. Friedrich, "Real-time gap impedance monitoring of dielectrophoretic assembly of multiwalled carbon nanotubes," *Applied Physics Letters*, vol. 92, no. 17, p. 173103, 2008.
- [148] M. T. Rabbani, M. Sonker, and A. Ros, "Carbon nanotube dielectrophoresis: Theory and applications," *Electrophoresis*, vol. 41, no. 21-22, pp. 1893-1914, 2020.
- [149] T. Müller *et al.*, "Trapping of micrometre and sub-micrometre particles by high-frequency electric fields and hydrodynamic forces," *Journal of Physics D: Applied Physics*, vol. 29, no. 2, p. 340, 1996.
- [150] M. P. Hughes and H. Morgan, "Dielectrophoretic trapping of single sub-micrometre scale bioparticles," *Journal of Physics D:* applied physics, vol. 31, no. 17, p. 2205, 1998.

- [151] J. Voldman, M. L. Gray, M. Toner, and M. A. Schmidt, "A microfabrication-based dynamic array cytometer," *Analytical chemistry*, vol. 74, no. 16, pp. 3984-3990, 2002.
- [152] J. Voldman, M. Toner, M. Gray, and M. Schmidt, "Design and analysis of extruded quadrupolar dielectrophoretic traps," *Journal* of electrostatics, vol. 57, no. 1, pp. 69-90, 2003.
- [153] S. Bhattacharya, T. C. Chao, and A. Ros, "Insulator-based dielectrophoretic single particle and single cancer cell trapping," *Electrophoresis*, vol. 32, no. 18, pp. 2550-2558, 2011.
- [154] G. Pendharkar et al., "An iDEP Based Single Cell Encapsulation Microfluidic Device Using Lift-Off Technique," in 2019 20th International Conference on Solid-State Sensors, Actuators and Microsystems & Eurosensors XXXIII (TRANSDUCERS & EUROSENSORS XXXIII), 2019: IEEE, pp. 2262-2265.
- [155] M. Oh, V. Jayasooriya, S. O. Woo, D. Nawarathna, and Y. Choi, "Selective Manipulation of Biomolecules with Insulator-Based Dielectrophoretic Tweezers," ACS applied nano materials, vol. 3, no. 1, pp. 797-805, 2020.
- [156] G. Zhou, M. Imamura, J. Suehiro, and M. Hara, "A dielectrophoretic filter for separation and collection of fine particles suspended in liquid," in Conference Record of the 2002 IEEE Industry Applications Conference. 37th IAS Annual Meeting (Cat. No. 02CH37344), 2002, vol. 2: IEEE, pp. 1404-1411.
- [157] X.-B. Wang, R. Pethig, and T. B. Jones, "Relationship of dielectrophoretic and electrorotational behaviour exhibited by polarized particles," *Journal of Physics D: Applied Physics*, vol. 25, no. 6, p. 905, 1992.
- [158] G. H. Markx, M. S. Talary, and R. Pethig, "Separation of viable and non-viable yeast using dielectrophoresis," *Journal of biotechnology*, vol. 32, no. 1, pp. 29-37, 1994.
- [159] Y. Huang, S. Joo, M. Duhon, M. Heller, B. Wallace, and X. Xu, "Dielectrophoretic cell separation and gene expression profiling on microelectronic chip arrays," *Analytical chemistry*, vol. 74, no. 14, pp. 3362-3371, 2002.
- [160] W. Waheed, A. Alazzam, B. Mathew, N. Christoforou, and E. Abu-Nada, "Lateral fluid flow fractionation using dielectrophoresis (LFFF-DEP) for size-independent, label-free isolation of circulating tumor cells," *Journal of Chromatography B*, vol. 1087, pp. 133-137, 2018.
- [161] X. Huang *et al.*, "Self-aligned sequential lateral field non-uniformities over channel depth for high throughput dielectrophoretic cell deflection," *Lab on a Chip*, vol. 21, no. 5, pp. 835-843, 2021.
- [162] I. Turcan and M. A. Olariu, "Dielectrophoretic manipulation of cancer cells and their electrical characterization," ACS Combinatorial Science, vol. 22, no. 11, pp. 554-578, 2020.
- [163] O. Zahedi Siani, M. Zabetian Targhi, M. Sojoodi, and M. Movahedin, "Dielectrophoretic separation of monocytes from cancer cells in a microfluidic chip using electrode pitch optimization," *Bioprocess and Biosystems Engineering*, vol. 43, no. 9, pp. 1573-1586, 2020.
- [164] A. T. Giduthuri, S. K. Theodossiou, N. R. Schiele, and S. K. Srivastava, "Dielectrophoretic characterization of tenogenically differentiating mesenchymal stem cells," *Biosensors*, vol. 11, no. 2, p. 50, 2021.
- [165] S. Afshar, A. Fazelkhah, E. Salimi, M. Butler, D. J. Thomson, and G. E. Bridges, "Dielectric properties of single cells subjected to heat shock using DEP cytometry," *IEEE Transactions on Microwave Theory and Techniques*, vol. 66, no. 12, pp. 5933-5940, 2018.
- [166] Z. Gagnon, J. Gordon, S. Sengupta, and H. C. Chang, "Bovine red blood cell starvation age discrimination through a glutaraldehydeamplified dielectrophoretic approach with buffer selection and membrane cross-linking," *Electrophoresis*, vol. 29, no. 11, pp. 2272-2279, 2008.
- [167] M. Hajari, A. Ebadi, M. J. F. Heydari, M. Fathipour, and M. Soltani, "Dielectrophoresis-based microfluidic platform to sort micro-particles in continuous flow," *Microsystem Technologies*, vol. 26, no. 3, pp. 751-763, 2020.
- [168] H. Huang *et al.*, "Stiffness-Independent Highly Efficient On-Chip Extraction of Cell-Laden Hydrogel Microcapsules from Oil Emulsion into Aqueous Solution by Dielectrophoresis," *Small*, vol. 11, no. 40, pp. 5369-5374, 2015.
- [169] M. Sun, P. Durkin, J. Li, T. L. Toth, and X. He, "Label-free onchip selective extraction of cell-aggregate-laden microcapsules

- from oil into aqueous solution with optical sensor and dielectrophoresis," *ACS sensors*, vol. 3, no. 2, pp. 410-417, 2018.
- [170] M. Sun, J. Xu, J. G. Shamul, X. Lu, S. Husain, and X. He, "Creating a capture zone in microfluidic flow greatly enhances the throughput and efficiency of cancer detection," *Biomaterials*, vol. 197, pp. 161-170, 2019.
- [171] A. M. White *et al.*, "Deep Learning-Enabled Label-Free On-Chip Detection and Selective Extraction of Cell Aggregate-Laden Hydrogel Microcapsules," *Small*, vol. 17, no. 23, p. 2100491, 2021.
- [172] I. Ertugrul and O. Ulkir, "Dielectrophoretic separation of platelet cells in a microfluidic channel and optimization with fuzzy logic," RSC Advances, vol. 10, no. 56, pp. 33731-33738, 2020.
- [173] G. M. Whitesides, E. Ostuni, S. Takayama, X. Jiang, and D. E. Ingber, "Soft lithography in biology and biochemistry," *Annual review of biomedical engineering*, vol. 3, no. 1, pp. 335-373, 2001.
- [174] H. A. Stone, A. D. Stroock, and A. Ajdari, "Engineering flows in small devices: microfluidics toward a lab-on-a-chip," *Annu. Rev. Fluid Mech.*, vol. 36, pp. 381-411, 2004.
- [175] Y. Wang, J. Wang, X. Wu, Z. Jiang, and W. Wang, "Dielectrophoretic separation of microalgae cells in ballast water in a microfluidic chip," *Electrophoresis*, vol. 40, no. 6, pp. 969-978, 2019.
- [176] M. A. Zaman, P. Padhy, W. Ren, M. Wu, and L. Hesselink, "Microparticle transport along a planar electrode array using moving dielectrophoresis," *Journal of Applied Physics*, vol. 130, no. 3, p. 034902, 2021.
- [177] T. Thorsen, S. J. Maerkl, and S. R. Quake, "Microfluidic large-scale integration," *Science*, vol. 298, no. 5593, pp. 580-584, 2002.
- [178] T. P. Hunt, D. Issadore, and R. M. Westervelt, "Integrated circuit/microfluidic chip to programmably trap and move cells and droplets with dielectrophoresis," *Lab on a Chip*, vol. 8, no. 1, pp. 81-87, 2008.
- [179] R. B. Fair, "Digital microfluidics: is a true lab-on-a-chip possible?," *Microfluidics and Nanofluidics*, vol. 3, no. 3, pp. 245-281, 2007.
- [180] Y. Piao, K. Yu, T. B. Jones, and W. Wang, "Electrical actuation of dielectric droplets by negative liquid dielectrophoresis," *Electrophoresis*, 2021.
- [181] I. Frozanpoor et al., "Programmable droplet actuating platform using liquid dielectrophoresis," *Journal of Micromechanics and Microengineering*, vol. 31, no. 5, p. 055014, 2021.
- [182] A. Isozaki *et al.*, "Sequentially addressable dielectrophoretic array for high-throughput sorting of large-volume biological compartments," *Science advances*, vol. 6, no. 22, p. eaba6712, 2020.
- [183] I. Frozanpoor, M. D. Cooke, V. Ambukan, A. J. Gallant, and C. Balocco, "Continuous Droplet-Actuating Platforms via an Electric Field Gradient: Electrowetting and Liquid Dielectrophoresis," *Langmuir*, 2021.
- [184] A. B. Fuchs *et al.*, "Electronic sorting and recovery of single live cells from microlitre sized samples," *Lab on a Chip*, vol. 6, no. 1, pp. 121-126, 2006.
- [185] B. Y. Park, L. Taherabadi, C. Wang, J. Zoval, and M. J. Madou, "Electrical properties and shrinkage of carbonized photoresist films and the implications for carbon microelectromechanical systems devices in conductive media," *Journal of the Electrochemical Society*, vol. 152, no. 12, p. J136, 2005.
- [186] A. Sajedi-Moghaddam, E. Rahmanian, and N. Naseri, "Inkjet-Printing Technology for Supercapacitor Application: Current State and Perspectives," ACS Applied Materials & Interfaces, vol. 12, no. 31, pp. 34487-34504, 2020.
- [187] P. Yang, L. Zhang, D. J. Kang, R. Strahl, and T. Kraus, "High-resolution inkjet printing of quantum dot light-emitting microdiode arrays," *Advanced Optical Materials*, vol. 8, no. 1, p. 1901429, 2020.
- [188] M. Heckele and W. Schomburg, "Review on micro molding of thermoplastic polymers," *Journal of Micromechanics and Microengineering*, vol. 14, no. 3, p. R1, 2003.
- [189] J. Giboz, T. Copponnex, and P. Mélé, "Microinjection molding of thermoplastic polymers: a review," *Journal of micromechanics and microengineering*, vol. 17, no. 6, p. R96, 2007.
- [190] H. Shaffee, J. L. Caldwell, M. B. Sano, and R. V. Davalos, "Contactless dielectrophoresis: a new technique for cell

manipulation, " $\it Biomedical\ microdevices,\ vol.\ 11,\ no.\ 5,\ pp.\ 997-1006,\ 2009.$